Gravity and Magnetic Investigations of the Deep Cove Intrusive, Cape Breton County, Nova Scotia

by

Richard W. Toews

Submitted in partial fulfillment of the
requirements of Bachelor of Science Degree with Honours
at
Dalhousie University
Halifax, Nova Scotia

March, 1978

DEPARTMENT OF GEOLOGY
DALHOUSIE UNIVERSITY
HALIFAX, NOVA SCOTIA
CANADA
B3H 4J1

DALHOUSIE UNIVERSITY, DEPARTMENT OF GEOLOGY

B.Sc. HONOURS THESIS

Author: Richard W. Toews

Title: Gravity and Magnetic Investigations of the Deep Cove Intrusive, Cape Breton County, Nova Scotia.

Signature of author

Date: March 15, 1978

Distribution License

DalSpace requires agreement to this non-exclusive distribution license before your item can appear on DalSpace.

NON-EXCLUSIVE DISTRIBUTION LICENSE

You (the author(s) or copyright owner) grant to Dalhousie University the non-exclusive right to reproduce and distribute your submission worldwide in any medium.

You agree that Dalhousie University may, without changing the content, reformat the submission for the purpose of preservation.

You also agree that Dalhousie University may keep more than one copy of this submission for purposes of security, back-up and preservation.

You agree that the submission is your original work, and that you have the right to grant the rights contained in this license. You also agree that your submission does not, to the best of your knowledge, infringe upon anyone's copyright.

If the submission contains material for which you do not hold copyright, you agree that you have obtained the unrestricted permission of the copyright owner to grant Dalhousie University the rights required by this license, and that such third-party owned material is clearly identified and acknowledged within the text or content of the submission.

If the submission is based upon work that has been sponsored or supported by an agency or organization other than Dalhousie University, you assert that you have fulfilled any right of review or other obligations required by such contract or agreement.

Dalhousie University will clearly identify your name(s) as the author(s) or owner(s) of the submission, and will not make any alteration to the content of the files that you have submitted.

If you have questions regarding this license please contact the repository manager at dalspace@dal.ca.

Grant the distribution license by signing and dating below.

_____ _____

Name of signatory Date

Table of Contents

List of Figures

Abstract

Gravity and magnetic surveys were conducted on the Deep Cove quartz monzonite intrusive to ascertain its subsurface configuration and, in particular, the attitude of its west contact with the surrounding Fourchu volcanic rocks.

Laboratory measurements of both intrusive and volcanic rock samples from Deep Cove indicate a density contrast of 0.10-0.15 $g.cm^{-3}$ and a magnetic susceptibility contrast of 1.5×10^{-3} measured in cgs units. The Koenigsberger Q-ratios of the samples are, in general, considerably less than unity. The expected anomalies caused by these contrasting properties are observed in the survey data.

Using a two-dimensional modelling computer program, models were developed which result in calculated gravity and magnetic anomalies that approximate the observed data. Gravity models suggest that the west contact of the intrusive is almost vertical, perhaps dipping steeply to the west. The calculated anomalies of magnetic models are less sensitive to the attitude of contacts.

Magnetic models require: (1) a greater susceptibility contrast than that measured in the laboratory and (2) a depth to the top of the 'magnetic body' of approximately 30 metres. These requirements possibly indicate weathering of ferrimagnetic minerals in the uppermost volcanic rocks.

Acknowledgements

I would like to sincerely thank Dr. John Peirce for his supervision during the course of this thesis, including the several days spent in the rain obtaining the oriented samples.

I would also like to acknowledge the suggestions of Dr. Jim Hall, Dr. Chris Beaumont and Dr. Marcos Zentilli of Dalhousie University, Dr. Charlotte Keen at Bedford Institute of Oceanography, Dr. Ken Howells at the Nova Scotia Research Foundation and Dr. John Riddell of Louisbourg Mines, Ltd.

I thank Dr. Allin Folinsbee and Brian MacIntyre of Bedford Institute of Oceanography for permission and assistance in using the modelling program, MAGRAV.

Thanks are also due to Jeff Clark of Dalhousie University for technicial assistance and instruction in the use of the equipment.

Special thanks are due Jane, my wife, for assistance in the field and for providing me moral support during the duration of this study.

I. Introduction

The Deep Cove quartz monzonite intrusive is located in south-eastern Cape Breton on the north shore of Gabarus Bay within the boundaries of Louisbourg National Park (Fig. 1). Numerous molybdenite occurrences can be found along the shoreline near Deep Cove especially in the siliceous dykes which intrude the Fourchu volcanic rocks. By a Federal-Provincial agreement, mineral rights for several areas within the park have been retained by the private sector and are currently held by Louisbourg Mines Ltd. Several exploration programs, involving geophysical, geochemical and drilling investigations, have been conducted on the property since 1962 indicating substantial quantities of low-grade base metal mineralization. Anomalous values of copper, molybdenum, bismuth and silver are associated with the intrusive. Alteration zones within the intrusive are similar to those found in porphyry copper deposits in the southwestern United States (Lehman, 1976; Hollister et al., 1974).

The nature of the western contact of the intrusive is of considerable interest as anomalous values of molybdenum and copper were found there in percussion holes drilled by United Asbestos Co. in 1971-72. Prior to 1976 this contact was considered to be fault-controlled. The evidence is a fault near the contact at the beach which strikes approximately 020° and dips 60-70° to the east. A diamond drill hole (Hole D.D.5 shown in Figure 5) was drilled in the

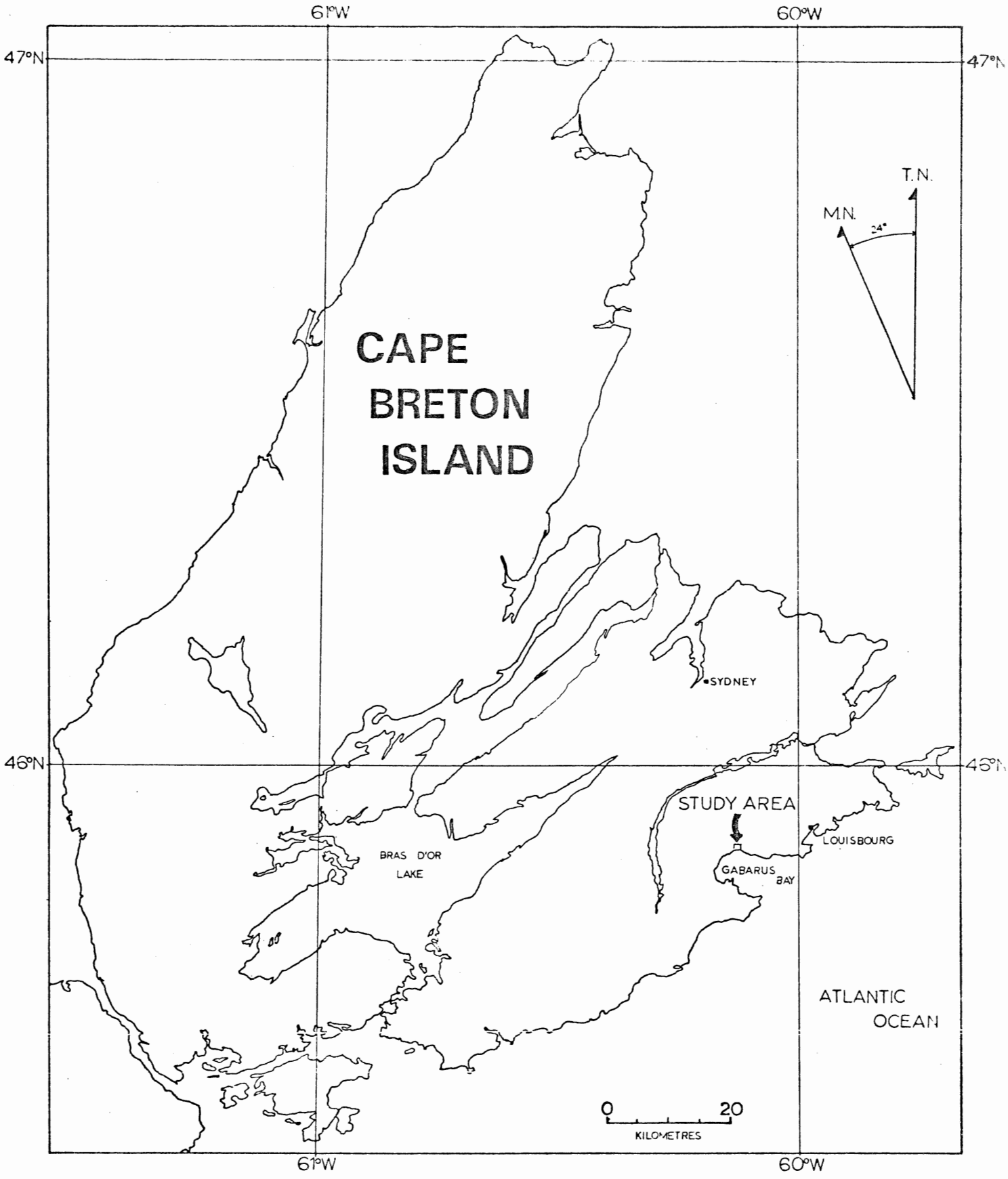

Figure 1. Location of study area.

quartz monzonite by St. Joseph's Exploration Ltd. towards 300° at -75°. The hole was designed to intersect an eastward dipping contact with a dip of 75° or less, but failed to intersect the volcanic country rocks, even though it extended to a depth of 180 metres. In addition, a trench dug across the contact just north of the access road does not expose a 'contact fault' (Sangster, 1976). Examination of the trench in 1977 revealed a gap of 2 or 3 metres between exposures of quartz monzonite and volcanic rocks. Therefore, the possibility of either a westward or steep eastward dipping fault contact can not be ruled out.

Magnetic and gravity surveys were conducted on the property. As granitic rocks are known to have lower average values of magnetic susceptibility and density than volcanic rocks (in this case, andesites), negative anomalies should be detected over the intrusive. An interpretation of these anomalies may provide an insight into the subsurface configuration of the intrusive and, hopefully, the attitude of the west contact.

II. General Geology

The geology of the southeastern coastline of Cape Breton, as described by Weeks (1954), is dominated by the volcanic-sedimentary sequence called the Fourchu Group. This group extends along the coast for nearly 80 kilometres from Little St. Esprit in the southwest to Scaterie Island in the northeast. It varies in width from about 2 to 15 kilometres.

The Fourchu Group consists principally of pyroclastic rocks. Lavas varying in composition from rhyolite to andesite are also present, but they are not as common as the pyroclastic rocks. Thin beds of shale and siltstone (up to two metres in thickness) are widely dispersed throughout the Fourchu Group (Bingley, 1967).

According to Weeks (1954) the Fourchu Group appears to grade conformably upwards into the sandstones and conglomerates of the Morrison River Formation. The Morrison River Formation, in turn, appears to grade into the MacCodrum Formation which has been established palaeontologically by Hutchinson (1952) to be of Lower Cambrian age. If these conformities indeed exist, the Fourchu Group is either late Hadrynian, as suggested by Weeks (1954), Wiebe (1972) and others, or it is lowermost Cambrian in age.

Granitic and dioritic plugs exist at various localities in southeastern Cape Breton. Several plugs, including the Deep Cove quartz monzonite, intrude the Fourchu Group near the west end of Gabarus Bay.

At Gillis Mountain a granitic pluton intrudes strata of known Middle Cambrian age (Hutchinson, 1952; Weeks, 1954; O'Reilly, 1977). Using the rubidium-strontium age dating technique, Cormier (1972) has obtained Devonian ages of 369 ± 25 m.y. for the Gillis Mountain intrusive and 350 ± 25 m.y. for the Deep Cove quartz monzonite. Both ages are based on a whole-rock - biotite pair isochron of a sample using a decay constant for ^{87}Rb of 1.39×10^{-11} yr^{-1}. These ages are considerably younger than those obtained elsewhere in Cape Breton. Cormier (1972) suggests that the biotites of these two samples have possibly been updated and that whole-rock ages should be attempted. O'Reilly (1977) maintains that, based on certain field relations, the plutonic rocks of southeastern Cape Breton are post-Middle Cambrian but pre-Devonian.

Gabbro and diabasic gabbro dykes are common and intrude all pre-Devonian rocks but are not found in Devonian or younger formations (O'Reilly, 1977).

III. Local Geology

In the vicinity of Deep Cove, outcrops along the shoreline are almost continuous, whereas inland they are relatively sparse. Glacial deposits with an average thickness of 5 to 10 metres cover most of the area with which this study is concerned. The inland outcrops and geology are shown in Figure 2.

Fourchu Group

The Fourchu volcanics near the Deep Cove intrusive are mainly fine-grained andesites. Some rhyolites and basic volcanics also occur in the area. The pyroclastic rocks are less common here than elsewhere in the Fourchu Group. The high magnetic relief as seen on aeromagnetic maps (see Figure 3) is most probably caused by the fact that the more basic volcanics possess a higher magnetite content than the andesites. Pyrrhotite exists in a few of the numerous dykes and faults in the area, also contributing to the high magnetic relief.

The Fourchu volcanics at Deep Cove have been subjected to a regional grade of metamorphism of the greenschist facies as evidenced by the development of chlorite, biotite and epidote (Sangster, 1976).

In the contact aureole surrounding the Deep Cove intrusive, the volcanics have been metamorphosed to hornfels, characterized by the development of biotite. Extensive silicification involving the introduction of granoblastic quartz also occurs in the contact rocks.

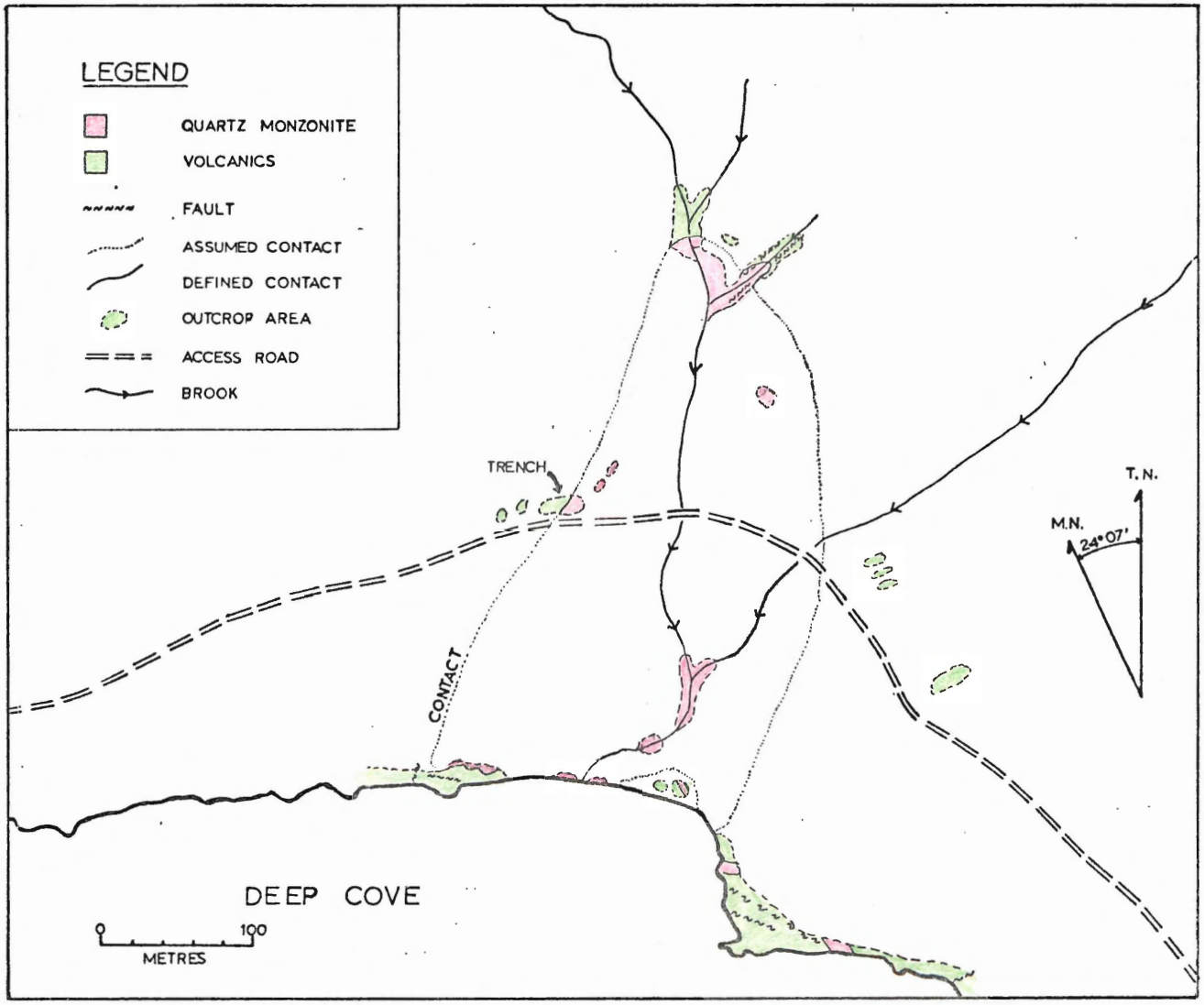

FIGURE 2. Geology Map of Deep Cove.

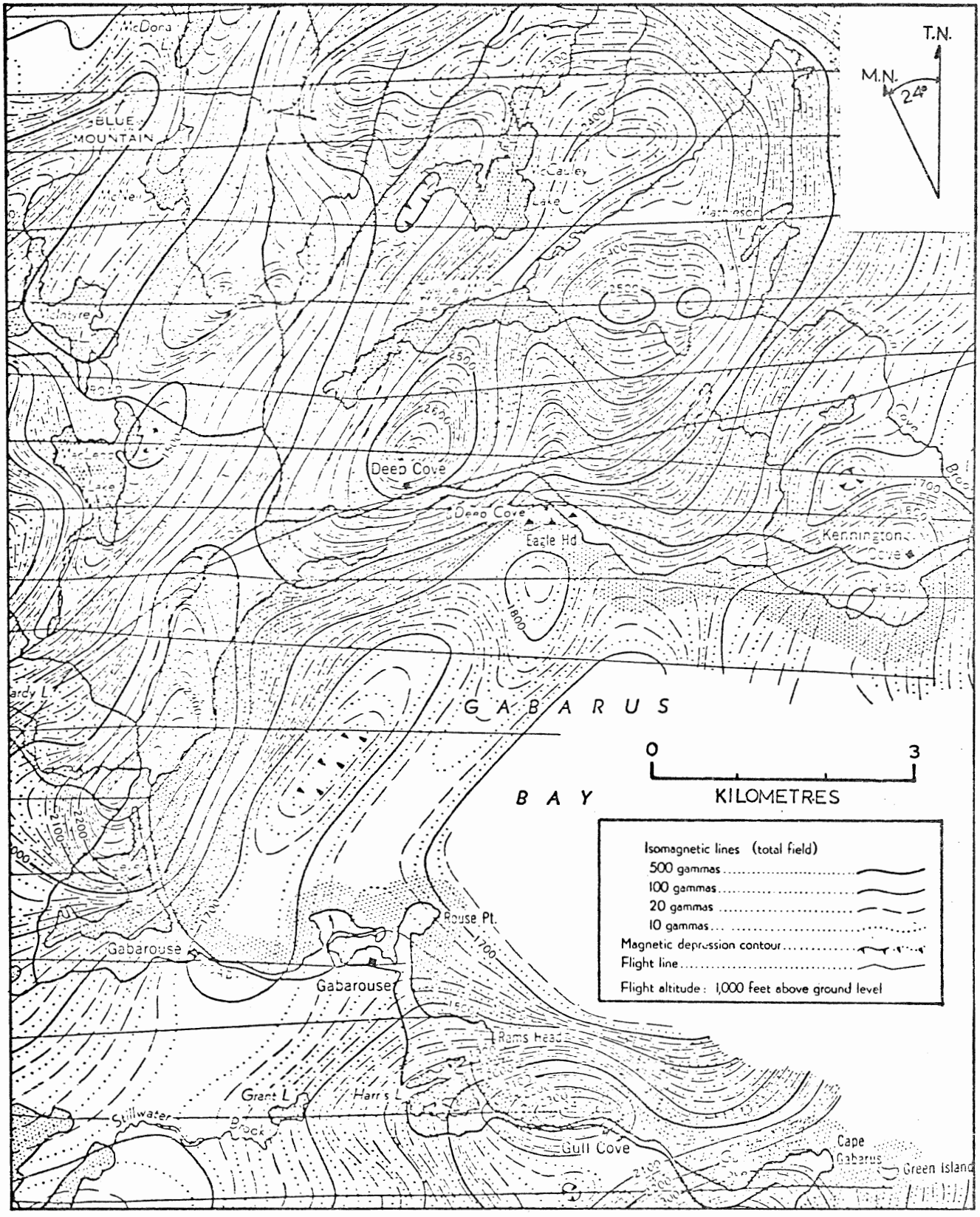

Figure 3. Aeromagnetic map of Deep Cove area (from Mira Map Sheet, 234G, Geol. Surv. Canada, 1955).

Deep Cove Quartz Monzonite Intrusive

Outcrops of the Deep Cove quartz monzonite intrusive occur along the several branches of Deep Cove Brook, along the beach where this brook enters Gabarus Bay and at several other locations as shown in Figure 2. The assumed contact between the volcanics and the intrusive depicted in this figure is based on the percussion holes drilled by United Asbestos Co. in 1971-72 and on magnetic data obtained by St. Joseph's Exploration Ltd. in 1976. This contact defines an intrusive with dimensions of approximately 175 metres by 350+ metres. The long axis strikes about 020°. In 1976 a trench was dug above the access road exposing rocks on either side of the western contact. The northern contact can be seen in several branches of the brook. It is not known if the intrusive extends out under Gabarus Bay. Shoreline exposures of the intrusive consist of mainly fine-grained quartz monzonite (with or without plagioclase phenocrysts) which intrude the volcanic country rocks as dykes. Several E - W striking faults can be seen on the point to the southeast of Deep Cove Brook. These factors tend to suggest that the extent of the intrusive under Gabarus Bay is limited.

The intrusive rocks are composed of plagioclase phenocrysts in a fine-grained matrix of quartz and orthoclase. Biotite, minor hornblende, and opaques constitute the mafic components (less than 10%). Such a rock is termed a quartz monzonite by the classification of Streckeisen (1967).

Structures

The Fourchu volcanics have been isoclinally folded, resulting in a regional strike of 020° to 035° with dips 60° to 80° to the east. The schistosity is sub-parallel to the regional strike.

Two major sets of faults and shears can be observed along the shoreline. One set tends to follow the regional strike while the other set runs roughly perpendicular to it. Most of these faults are considered to have only small relative displacements (Bingley, 1967). In general, they appear to have first developed in the volcanic rocks before the emplacement of the quartz monzonite, and post-intrusive tectonic movement has since extended them into the quartz monzonite (Riddell, 1973).

IV. Field Work

Survey Line

Several criteria were considered in choosing the survey line. The elevation of the ground increases moderately from the shoreline to the access road which is an average of 10 to 20 metres above sea level. North of the road the terrain is much steeper, climbing to an elevation of approximately 80 metres where it levels into a plateau. The access road runs almost perpendicular to both the topographic gradient and the assumed contacts, approximately bisecting the long axis of the intrusive. A gravity survey requires accurate levelling, which would be difficult if conducted on the steeper slopes. Although the beach would provide a relatively level line, the nature of the intrusive here and the uncertainty of its southern contact would complicate the geophysical interpretation. Therefore, the survey line followed the access road. There were 34 stations spaced at 20 metres measured by steel tape. Care was taken to keep the stations as far as possible from steep embankments to reduce the terrain effects. The station locations are shown in Figure 4.

The level survey was conducted using a Wild N2 Level of Dalhousie's Engineering Department. The elevation difference between any two stations was determined to within 3 mm corresponding to an error in relative gravity of less than 10^{-3} mgals. The station elevations relative to Station # 1 are listed in Appendix I.

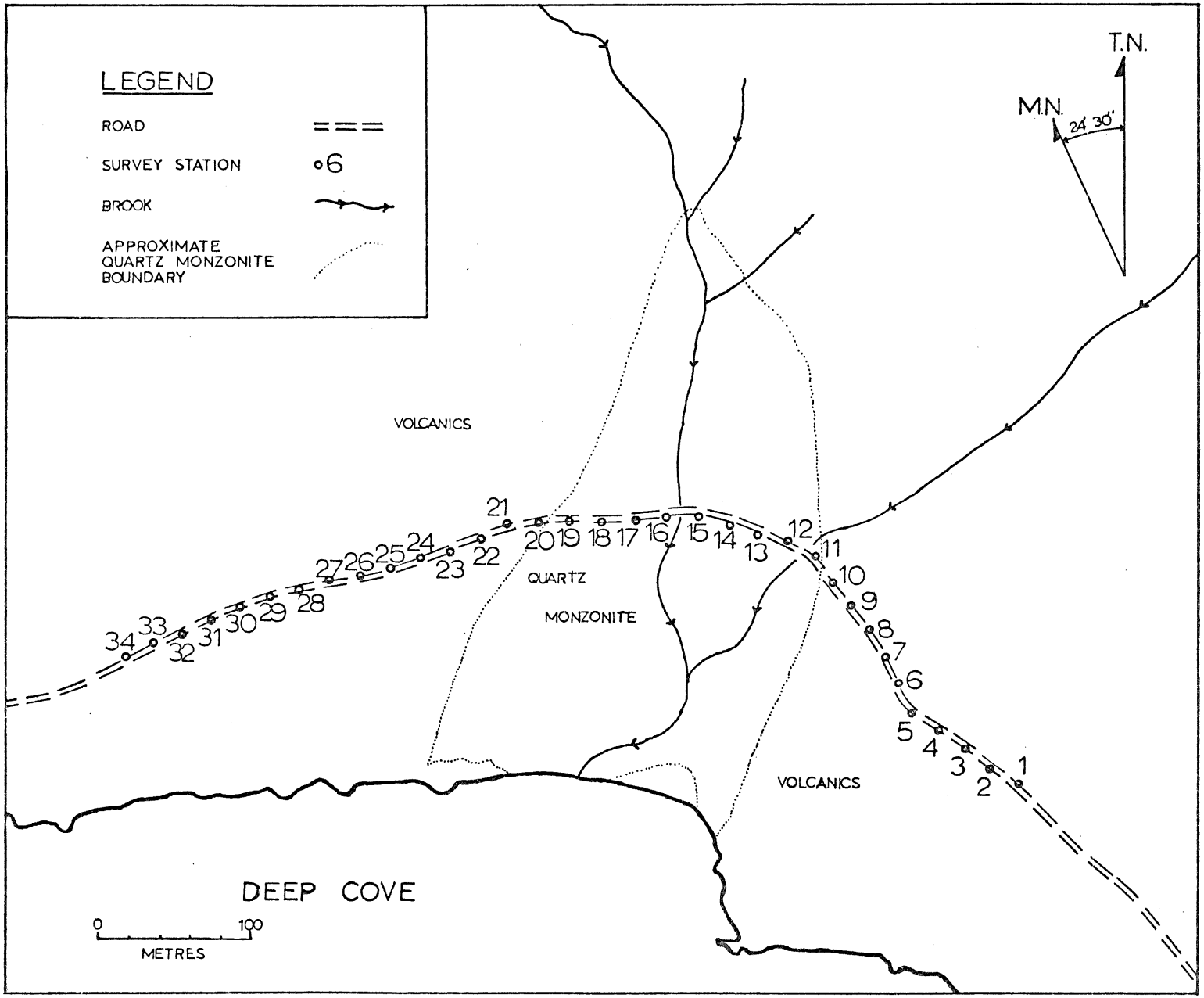

FIGURE 4. Survey Station Locations.

Gravity Survey

Gravity readings were taken on a Worden Gravity Meter courtesty of the Dalhousie Geology Department. The Worden readings were converted to milligals by using the most recent (March, November, 1977) calibration constant for the gravity meter of 0.4145 ± 0.05 mgals per dial division. Base stations were established to determine a drift curve for the gravity meter while the survey was in progress. Most of the base station readings were made within 30 minute intervals, with a maximum of 40 minutes between readings. The maximum drift rate obtained for the meter in the survey was 0.4 mgals/hr. The drift curve is shown in Appendix II. On the day the survey was conducted, the weather was cloudy. Occasional sunny periods may have caused some of the variations on the drift curve. A slight breeze caused some difficulty in reading the meter dial. The meter was set on a bowl-shaped tripod which straddled the 'station stone' in a consistent manner at each station to reduce additional adjustments to relative elevations between stations.

The survey was attempted a second time; however, half-way through the second survey the illumination light malfunctioned and therefore this survey was not completed. Comparison of the initial survey readings with those obtained from the second survey indicates a standard deviation of 0.10 mgals for each station's gravity.

Magnetometer Survey

This survey was done with a Scintrex MP-2 Proton Precession Magnetometer owned by the Dalhousie Geology Department. Individual

readings for this instrument are supposedly accurate to ± 1 nanotesla (gamma). Base stations were maintained and a drift curve calibrated. The maximum observed drift was 16 nanotesla, whereas the average variation between adjacent stations was about 300 nanotesla. Nevertheless the readings were corrected for drift.

Sampling

A total of forty-five samples were collected in the field and an additional nine samples (samples # DC46-54) were obtained from core drilled by St. Joseph's Exploration Ltd. in 1976. Fifteen oriented samples (samples # DC26-45, excluding DC36, 37 and 40-42) were obtained from outcrops using a portable drill. The samples were oriented relative to geographic landmarks and magnetic North using a palaeomagnetic orienting tool and a Brunton compass. All but two or three field samples were taken from outcrops and attempts were made to obtain as fresh a sample as possible. Sample locations are shown in Figure 5.

Whether or not these samples are a representative suite is questionable. Because of the paucity of outcrops, two or more samples were often taken from one outcrop. Oriented samples were taken in pairs to judge the variability in the magnetic properties. A high concentration of samples was taken in the trench near the western contact.

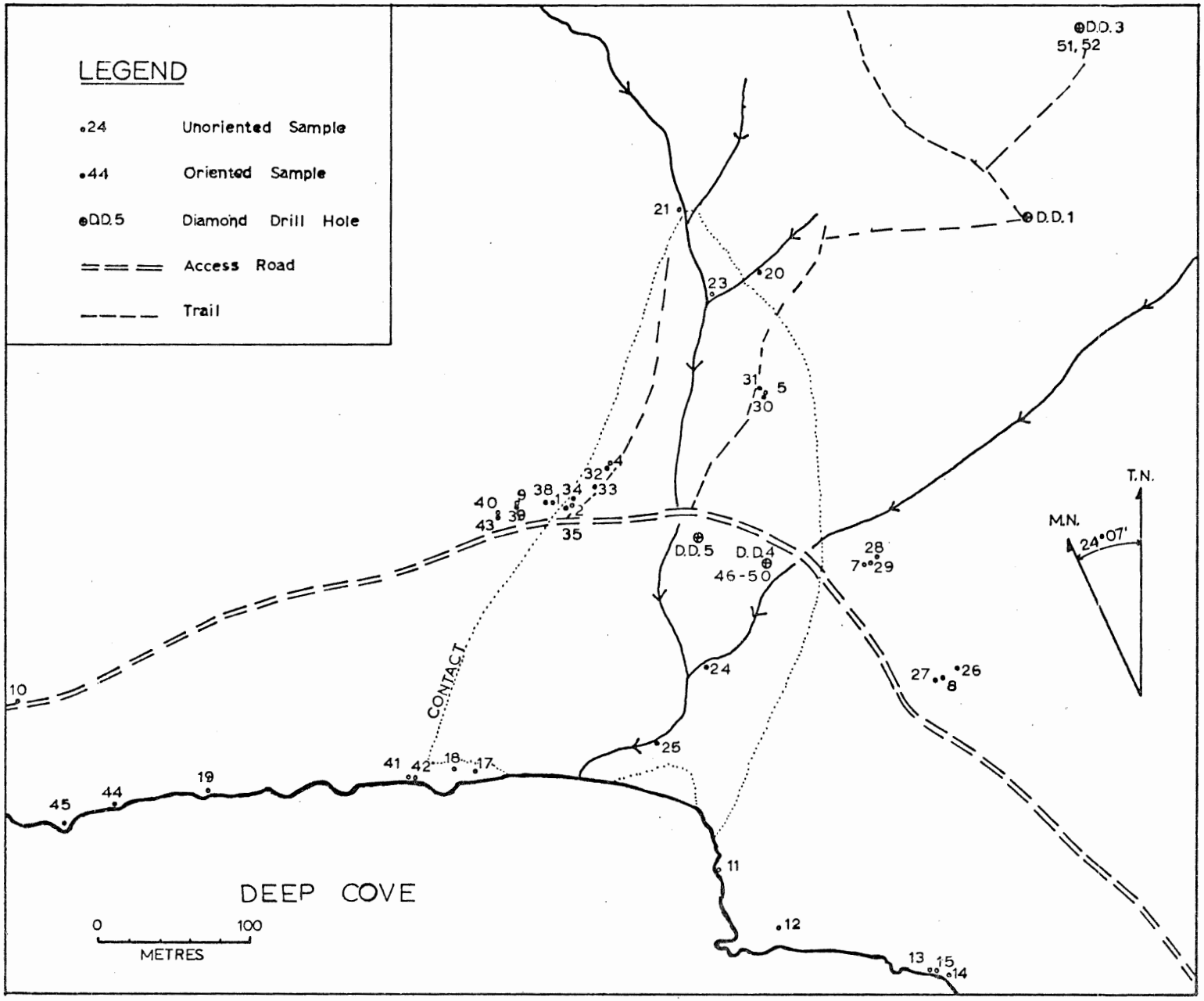

FIGURE 5. Sample Locations.

V. Laboratory Procedures and Deductions

Density Determinations

Samples were prepared for weighing by first chipping off the weathered surfaces with a hammer where possible and then scrubbing with a wire brush to remove loose fragments. Before weighing, they were dried in an oven for about 18 hours at 50°C. The samples were weighed using a balance beam scale. They were then allowed to soak overnight and reweighed suspended by a thin nylon wire in distilled water. Corrections were made for the weight of the wire when suspended in the water. The density of each sample was calculated using the formula:

$$\text{Density of sample} = \frac{\text{Dry weight of sample}}{\text{Dry weight-wet weight}} \times (\text{density of distilled water at } 20°C) \quad (1)$$

Considering the uncertainties involved, the densities were determined to within $\pm$ 0.01 g cm^{-3}. The sample densities are listed in Appendix III.

Histograms of the densities of the two major rock types are shown in Figures 6 and 7. A best estimate of the average density of the quartz monzonite is 2.63 $\pm$ 0.01 g cm^{-3}. An estimate of the average density of the volcanics is, however, less straightforward. The densities range from 2.65 to 3.03 g cm^{-3}. The bulk of the samples cluster around 2.73 g cm^{-3}. Many of these samples were taken within 40 metres of the intrusive and may not give a representative density of the Fourchu volcanic rocks as they occur in the siliceous aureole. Three

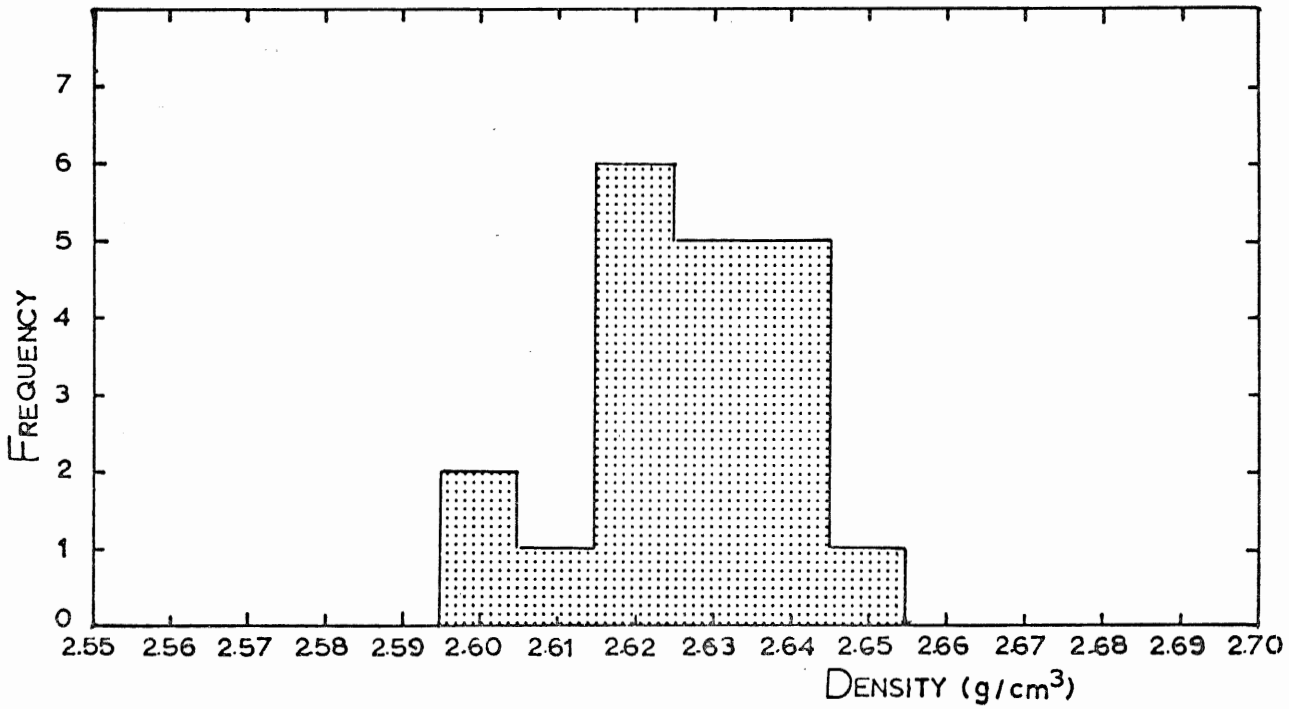

Figure 6. Histogram of densities of 20 quartz monzonite samples. Average density = 2.63 g cm^{-3}.

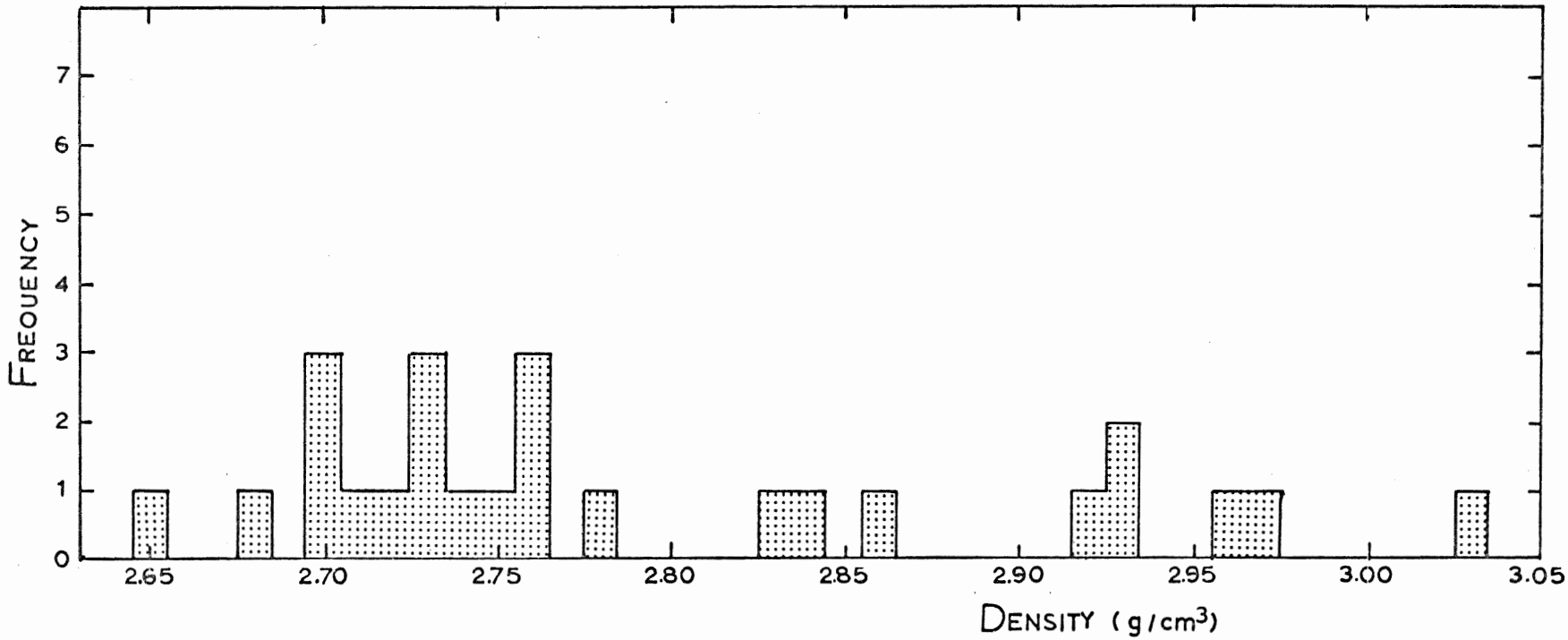

Figure 7. Histogram of densities of 24 volcanic samples, illustrating considerable variability. Average density = 2.78 g cm^{-3}.

of the six samples with densities greater than 2.90 g cm^{-3} were collected from a single outcrop about 65 metres east of the intrusive (samples DC8, 26 and 27). An additional sample (DC12; density = 2.96 g cm^{-3}) was collected on the beach on strike with this outcrop. These samples may represent a single basic unit within the volcanics. Taking the above considerations into account, the average density of the volcanic rocks is probably between 2.73 g cm^{-3} and 2.78 g cm^{-3}.

Magnetic Data Determinations on Oriented Samples

To determine the amount of remanent magnetization in the samples (especially the volcanics), most of the oriented samples were spun on a spinner magnetometer at Dalhousie University. The samples were stepwise demagnetized in alternating fields of varying strengths, depending on the stability of the remanent vectors. No consistency of residual magnetic vectors was apparent between samples, even though some of them had been adjacent to one another in situ. The results are summarized in Appendix IV.

The magnetic susceptibilities of these samples were measured on an inductance bridge which is capable of measuring susceptibilities as small as 10^{-5} in cgs units. (Susceptibility is a dimensionless ratio, but its magnitude depends on the units of measurement, the susceptibility of SI units being larger than the susceptibility in cgs or emu units by a factor of 4π). In most of the samples, with the exception of DC45, the Koenigsberger Q-ratios are considerably less than unity, indicating that the dominant magnetic vector due to the rock as measured in the field results from the induced magnetization caused by

the present magnetic field of the earth. Therefore, the remanent effect has been neglected, and the variable palaeomagnetic directions contribute a negligible amount to the magnetic anomaly.

The susceptibilities of the quartz monzonite samples were, in most cases, too small to measure. The susceptibilities of the volcanic samples, however, averaged about 1.5×10^{-3} in cgs units, which is at least 100 times greater than the susceptibility of the quartz monzonite. These values of the susceptibilities fall within the normal ranges listed for the two rock types (Telford et al., 1976, p. 121: Dobrin, 1976, p. 492).

VI. Gravity Reductions

Free-air Corrections

Most gravity meters are designed to measure variations in the acceleration due to gravity. The acceleration due to gravity, g, is actually a vector directed towards the centre of the earth, but the vector notation is often dropped and g is usually given as:

$$g = \frac{GM_e}{R_e^2} \tag{2}$$

where G is the universal gravitational constant
M_e is the mass of the earth
R_e is the distance to centre of the earth

The magnitude of g is approximately 9.8 m sec^{-2} = 980 cm sec^{-2}. The unit of acceleration of gravity, 1 cm sec^{-2}, is called 1 gal after Galileo. As variations of the earth's surface are often very much smaller than 1 gal, units of milligals (mgals) are commonly used in gravity work.

To obtain the variation of gravity with altitude, equation (2) is differentiated with respect to R_e, resulting in:

$$dg_{FA} = \frac{-2g}{R_e} dR_e \tag{3}$$

This is called the free-air correction an amounts to 0.3086 mgals/metre near mid-latitudes. It is added to the field reading if the station is above datum.

Bouguer Corrections

When calculating the free-air correction, the slab of material between the station and the datum plane was ignored. The Bouguer gravity effect, dg_B, derived from Gauss' Theorem, is

$$dg_B = 2 \pi G \sigma dR_e \qquad (4)$$

where σ is the density of the slab

Since the effect of the slab above datum is to increase the gravity readings, this correction must be subtracted from the field readings (if the station is above datum). By inserting the constants into (4), the numerical value of this correction becomes -0.04193 mgals/metre. The Bouguer correction can be combined with the free-air correction in:

$$dg_{FA} + dg_B = (0.3086 - 0.04193\sigma)\ h \qquad (5)$$

where h is the height of the station above datum

These corrections were applied to the observed gravity using the elevation of Station # 1 as datum. The density of the material, σ, between each station and datum was not known accurately. However, by correlating the topography to the observations, using the Spearman rank correlation coefficient (Mendenhall, 1971, p. 388+, Scientific Subroutine Package, subroutine SRANK) for different densities, a density of 2.00 g cm^{-3} was selected for the Bouguer correction. Correlation was actually performed on the height of the stations versus the deviation of the observed anomaly from the smoothed anomaly (see

Figure 9). The highest station was 14 metres above datum and the average thickness of the glacial deposits was 5 to 10 metres. The density of this slab of material would, therefore, be somewhat less than that of the underlying rock. In addition, careful weighing of the 1972 percussion hole drillings (in the quartz monzonite) resulted in an average mass deficiency of over 30% of what would be expected (J. E. Riddell, pers. comm.). It is therefore possible that due to weathering, fractures, and cavities the upper rock itself may have an overall density less than that obtained on samples in the laboratory. Consequently, the value of $\sigma = 2.00$ g cm^{-3} for the Bouguer correction is not unreasonable.

Terrain Corrections

If the terrain near a station is very irregular, corrections should be made for the upward attraction caused by hills above the station and the lack of downward attraction caused by valleys below the station. In either case, the terrain corrections are added to the field readings.

Terrain corrections were attempted using the technique of Hammer (1939). Circular charts were used, having compartments of increasing size and with corresponding tables (Hammer, 1939, Douglas and Prahl, 1972) that give the effect of each compartment as a function of its average elevation above or below the station. The chart was then moved to the next station and the process repeated. The elevations of the compartments near a station could not be estimated from

the topographic maps available (National Parks 1:7200 Map, 1962, and Mira Map Sheet, Department of Energy, Mines and Resources, Topographic Map 11F/16, 1:50000, 1975). The field notes were, therefore, used to estimate the terrain corrections near a station. The zones further away from the stations appear only to have the effect of increasing the regional gradient from east to west, because the topography becomes progressively steeper to the west of the survey area. Because the terrain corrections from the distant compartments were contained within the local regional gradient, they were removed with the regional trend. The terrain corrections from the nearby compartments for stations near steep embankments were, however, added to the observed readings.

Removal of Regional Gradient and Anomaly Smoothing

The station locations were projected onto a straight line at 018° which runs roughly perpendicular to the long axis of the intrusive. The corrected observations were then plotted versus the projected station locations (Figure 8) and the regional gradient removed. The regional gradient was approximated by the method of least squares (Mendenhall, 1971, p. 264+), fitting a straight line through the points furthest from the intrusive (the values at Stations # 1-7 and 26-34 were used). Once the regional gradient was removed, a smoothed curve (Figure 9) was fitted to the resulting data using a cubic spline smoothing computer program (Reinsch, 1967; International Mathematical and Statistical Libraries, Subroutine ICSSCU, 1977). A standard

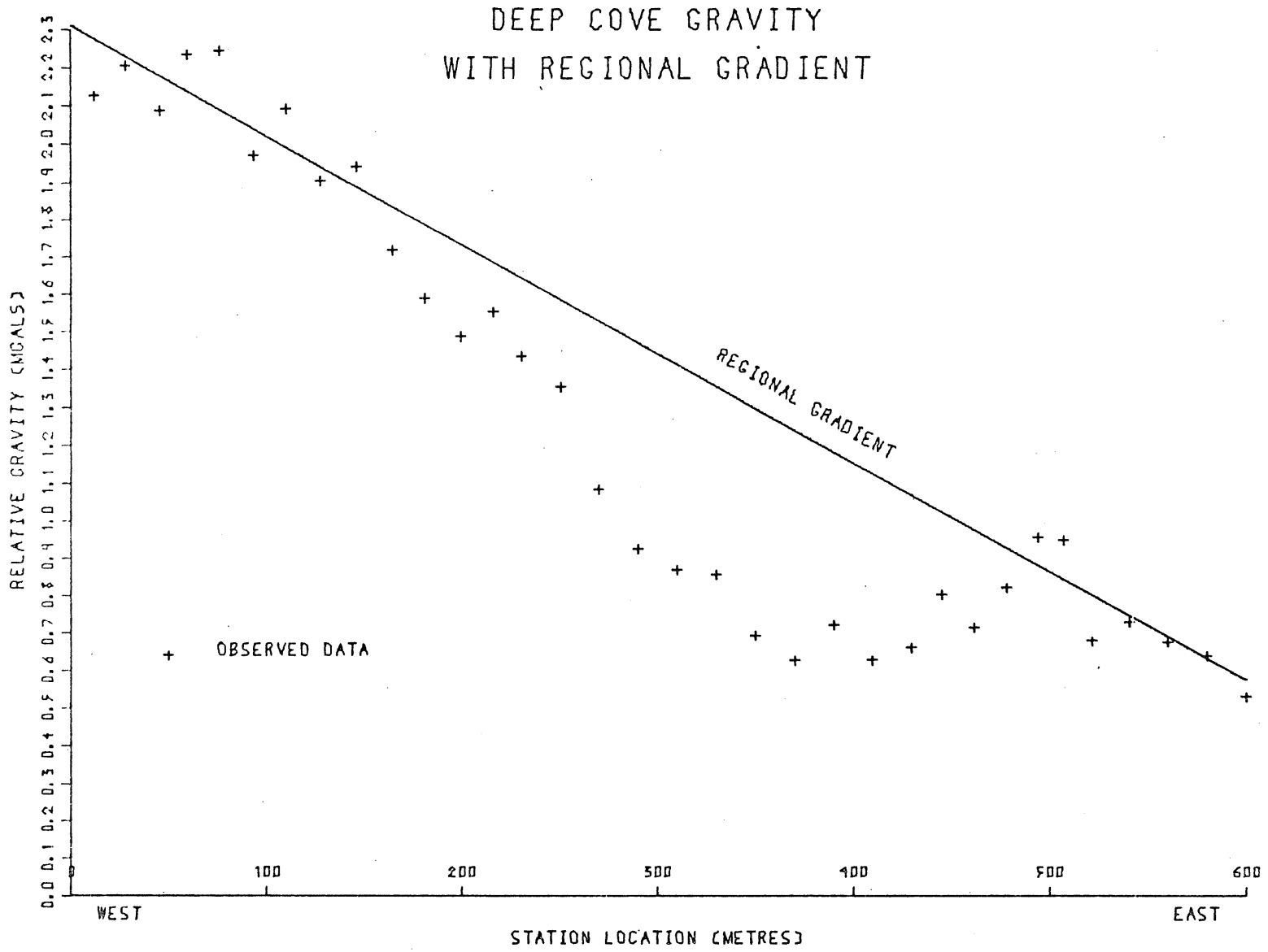

Figure 8. Observed gravity with regional gradient.

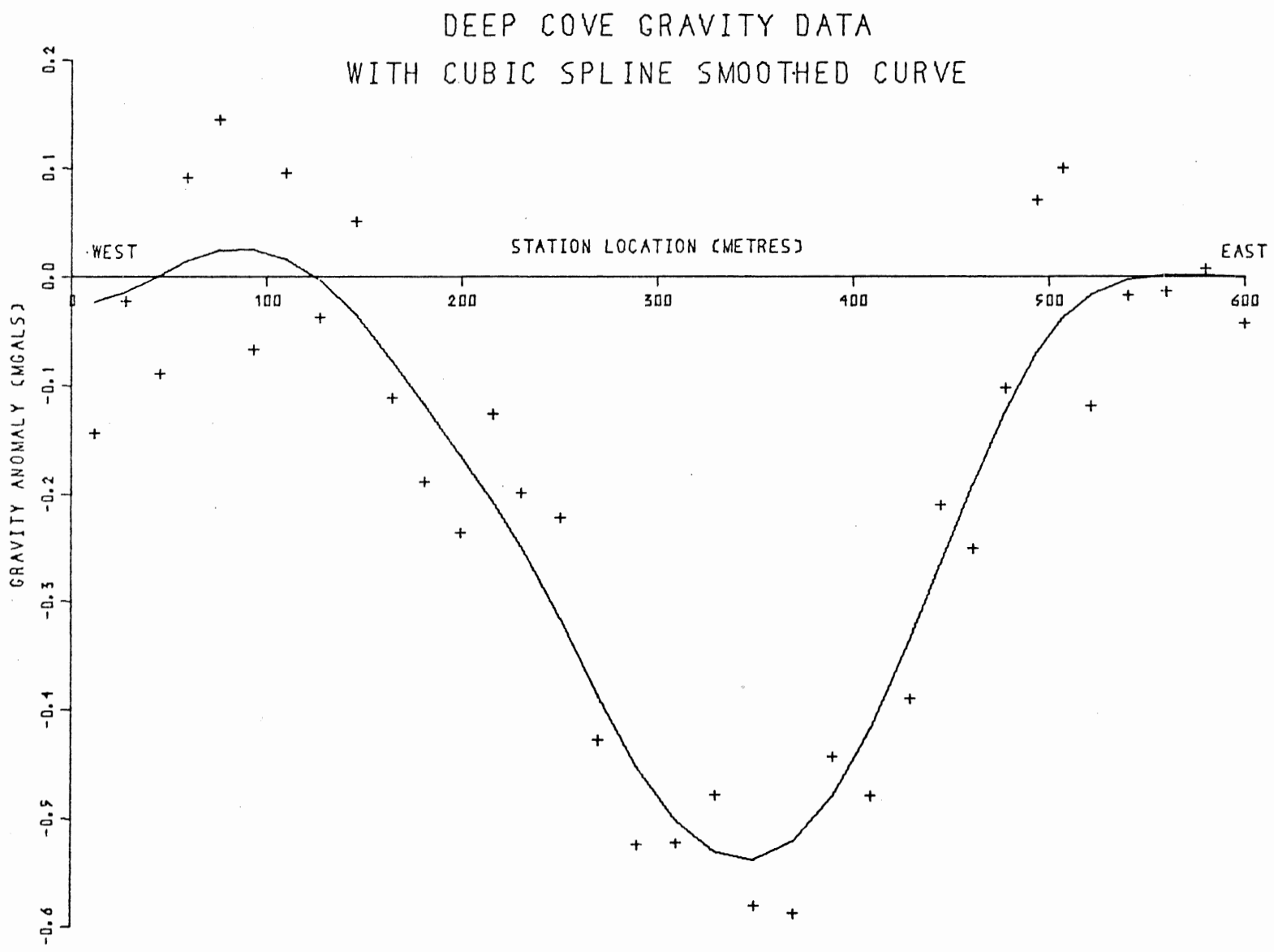

Figure 9. Cubic spline smoothed curve through Deep Cove gravity data using a weighting factor for the data corresponding to a standard deviation of 0.08 mgals.

deviation of 0.10 mgals, obtained from comparing readings of the first and second gravity surveys, was first used as a weighting factor for the data, but the resulting curve appeared to be oversmoothed. A weighting factor corresponding to a standard deviation for the data of 0.08 mgals resulted in a smoothed curve which best represented the data and was therefore used. As the second derivative of the spline function at Stations # 1 and 34 would be considered to be zero by the smoothing program, several fictitious points along the regional gradient were introduced at each end of the line. These fictitious points, however, have the somewhat negative effect of forcing the smoothed curve towards the regional gradient near the end points.

VII. Magnetic Reductions

Diurnal variations of the earth's magnetic field were removed from the field observations by a drift curve (see Appendix II). On the day the survey was conducted the earth's magnetic field was relatively stable, as indicated by the 16 nanotesla observed drift.

The magnetic observations with the regional gradient are shown in Figure 10. The regional gradient was estimated using a procedure similar to the gravity case. Because of the nature of the anomaly curve, the least squares line through observations at Stations # 1-3 and 20-34 was assumed to be the regional gradient. It was removed and the resulting data were fitted with a cubic spline function using a weighting factor of 175 nanotesla (see Figure 11). Even though the short wavelength magnetic variations are probably real, in that little error exists in the value of the magnetic field measured at a station at a particular time, the smoothing curve allows for simpler interpretative models which are more relevant to the problem at hand.

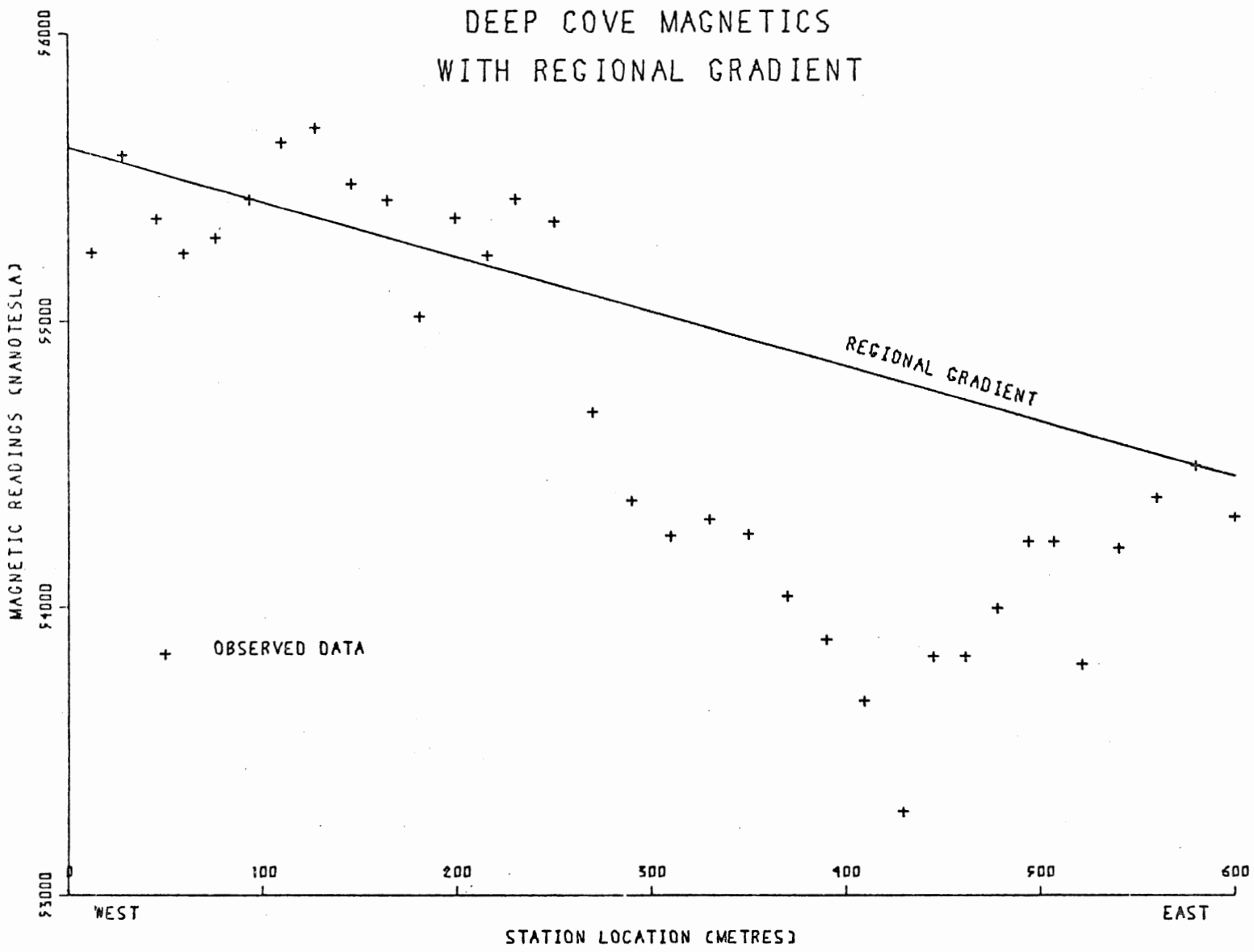

Figure 10. Observed magnetics with regional gradient.

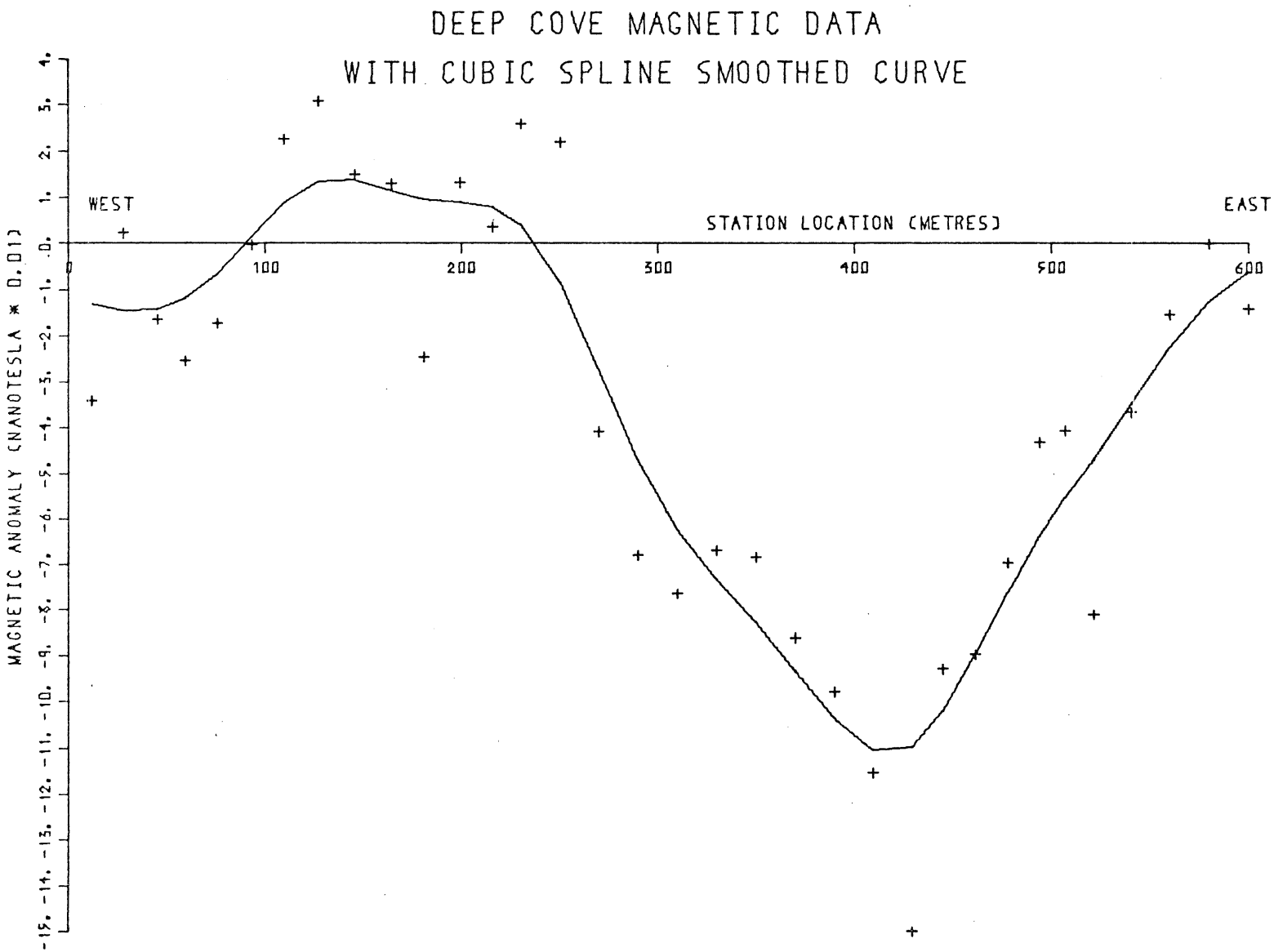

Figure 11. Cubic spline smoothed curve through magnetic data using a weighting factor for the data of 175 nanotesla.

VIII. Interpretation of Data

Both the gravity and magnetic interpretations are based on potential field theory. Unfortunately, an infinite number of configurations of subsurface sources can result in identical gravity (and magnetic) data at the surface. The 'inverse problem' lacks uniqueness and additional geological information is necessary to constrain the models used to explain the surface data. The principles of potential field theory are discussed in some detail by Grant and West (1965, p. 210-234).

Modelling was done using a computer program called MAGRAV owned by the Bedford Institute of Oceanography (BIO). The program has been developed at BIO to calculate the gravity and magnetic effects of subsurface two-dimensional density and magnetization configurations. It is an interactive program designed for use on Tektronix 4000-series graphics terminals using the PLOT10 system. MAGRAV was written by I. Wells and R. T. Haworth at BIO based on the work of Talwani *et al.* (1959).

As the survey line passed through the approximate centre of the intrusive perpendicular to the long axis and the length was several factors greater than the width, a two-dimensional model represents the three-dimensional body to a first order.

The MAGRAV program requires evenly-spaced stations readings. The distances between survey stations had been projected onto a line 588

metres long at 018° and were no longer 20 metres in most cases. To modify the anomaly points to equal-spaced intervals, the smoothed curves of Figures 9 and 11 were interpolated at 20 metre intervals reducing the number of 'observations' from 34 to 30. To make the line 600 metres in length for convenience, a 31st observation point was created with a value along the regional gradient.

Gravity Models

Geological constraints to subsurface models are limited. The surface locations of the east and west contacts are fairly accurately known from percussion hole drilling. The location of the western contact at the access road is substantiated by the trench. The average density contrast between the volcanics and the quartz monzonite has to be estimated because of the variability of the densities of the volcanics.

A value in the range of 0.10-0.15 g cm^{-3} was used while modelling. Only simple density configurations were attempted. Since the western contact was of greater interest, efforts were made to ascertain the effects that varying its angle had on the calculated anomalies.

The gravity anomaly of each model was first calculated; then the model was adjusted by varying the depth, shape and density parameters so that the calculated anomaly more closely matched the observed anomaly. The observed anomaly had to be shifted up or down in order to overlay the calculated anomaly for direct comparison.

At first, a model with rectangular cross-section was attempted. In order to obtain an anomaly which approximately fitted the shape and size of the observed anomaly, a density contrast between the intrusive and the country rock of 0.12 g cm^{-3} was required for the model. The depth of the body required for this model was 1.4 km. Figure 12 shows this model with its resulting gravity anomaly.

Models DC-2 (Figure 13) and DC-3 (Figure 14) illustrate the effect of varying the angle of the western contact. The best fit of the observed to calculated anomalies occurs when the contact is allowed to dip very steeply to the west as in Model DC-2. It should be noted that there is only a small angular difference of the west contact involved in Models DC-1, DC-2 and DC-3, although the horizontal exaggeration makes it seem much greater.

Model DC-4 (Figure 15) incorporates the denser unit ($\sigma > 2.90$) which was sampled to the east of the intrusive. This unit may be approximated by a two-dimensional body dipping steeply towards the east.

Some modelling observations are:

1) None of the calculated anomalies of models attempted are able to match the observed anomaly near the end points of the survey line. This is probably because the smoothed curve is forced towards the regional gradient near the end points.

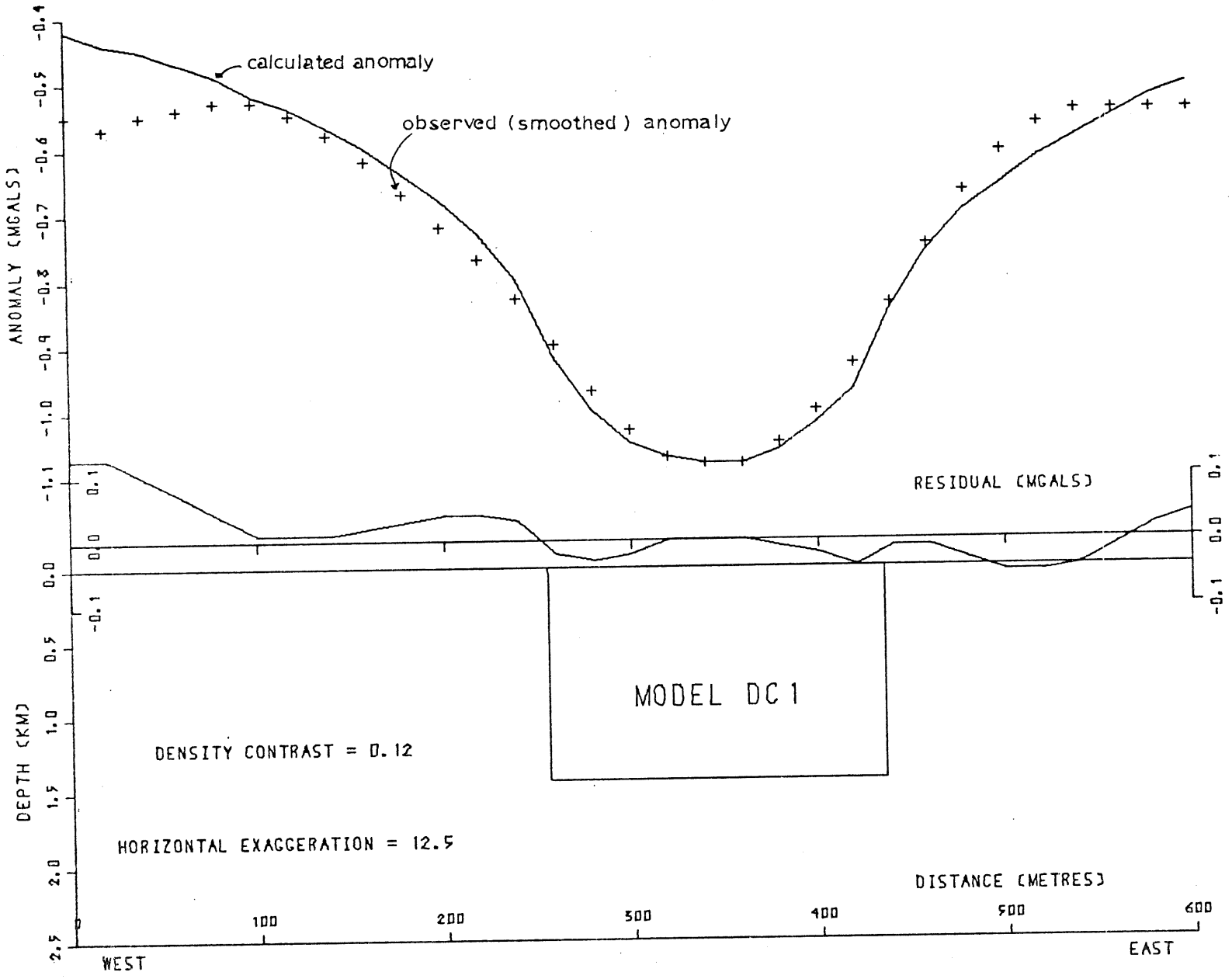

Figure 12. Gravity Model DC1, with vertical west contact.

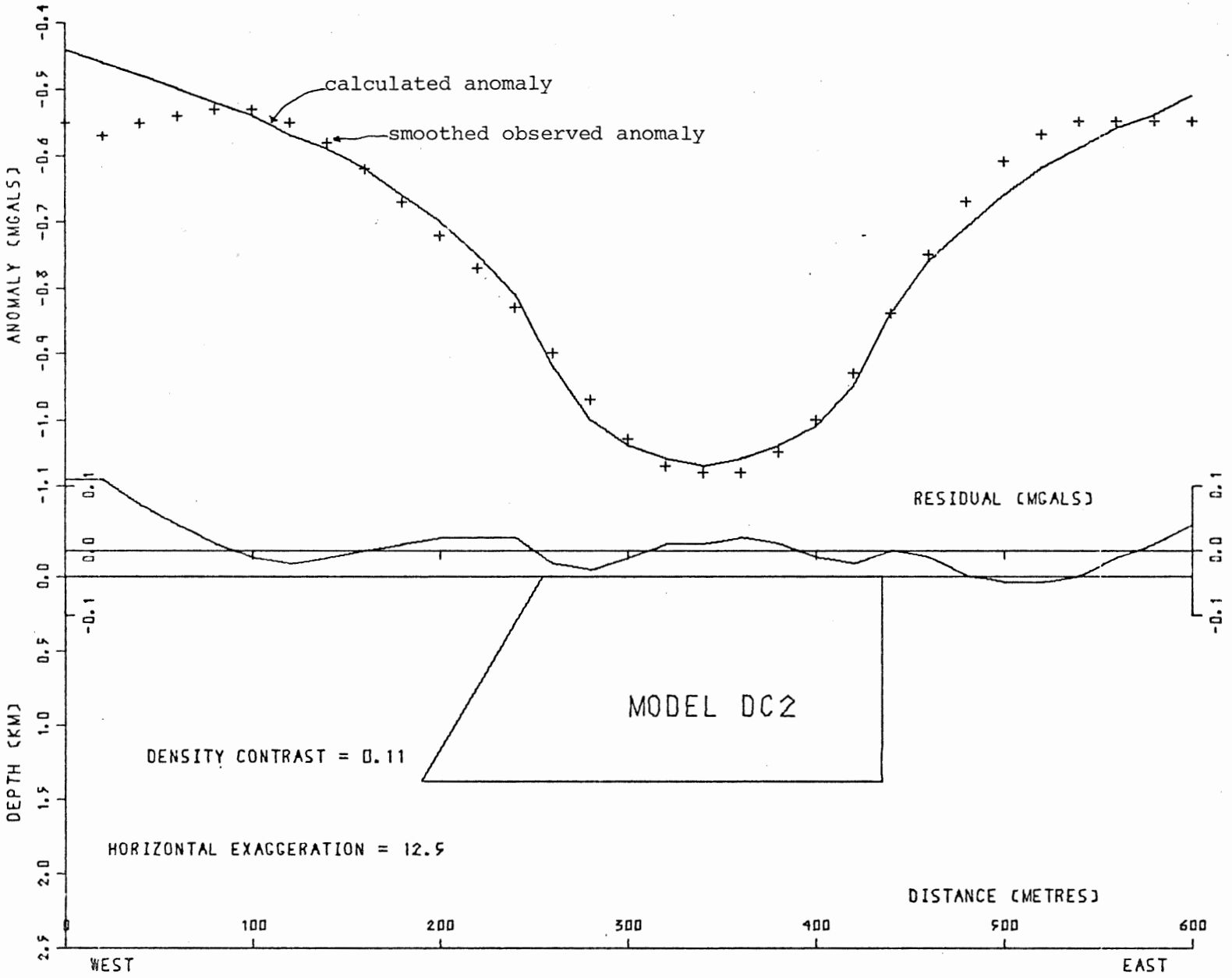

Figure 13. Gravity Model DC2, with west contact dipping steeply to the West.

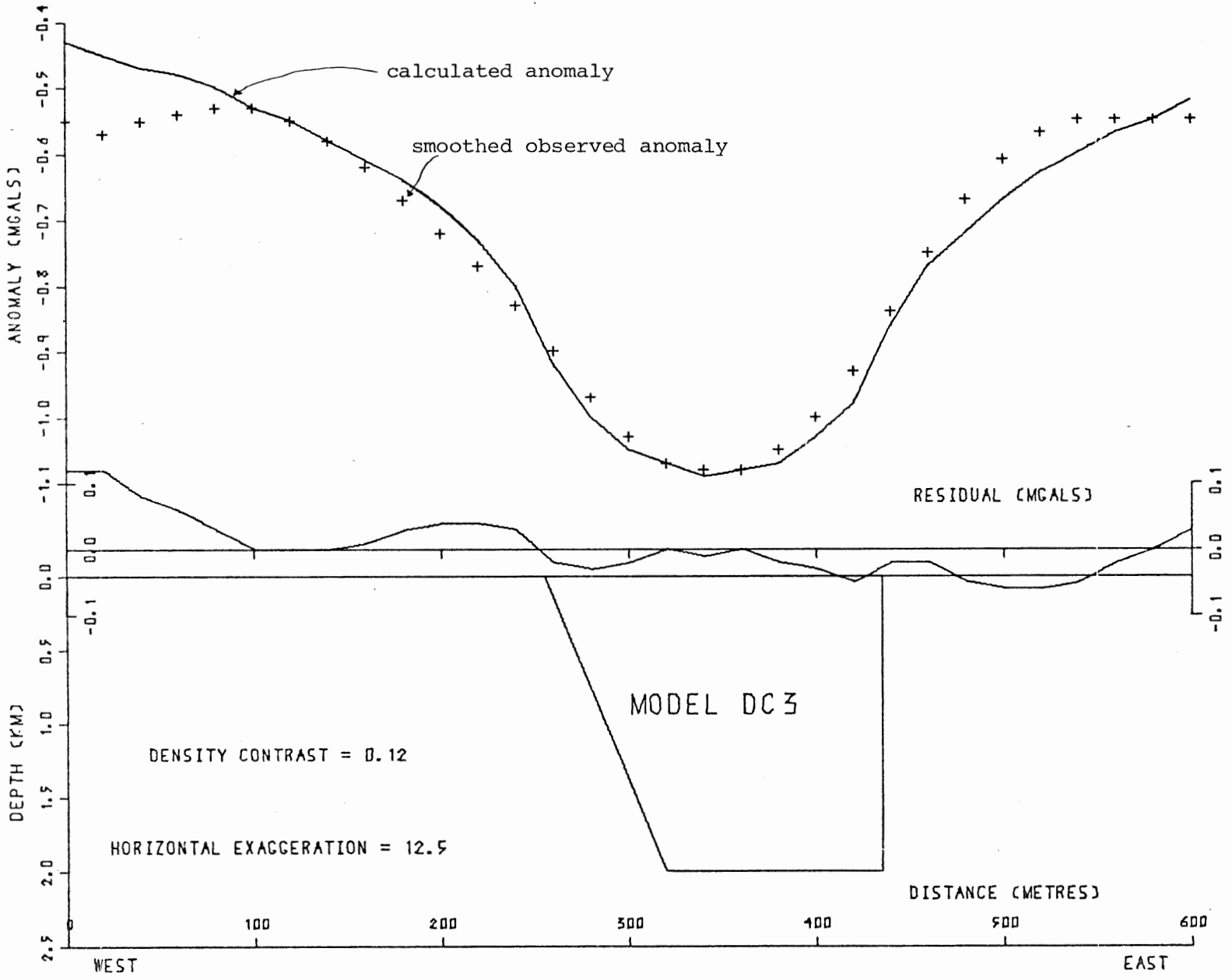

Figure 14. Gravity Model DC3, with west contact dipping steeply to the East.

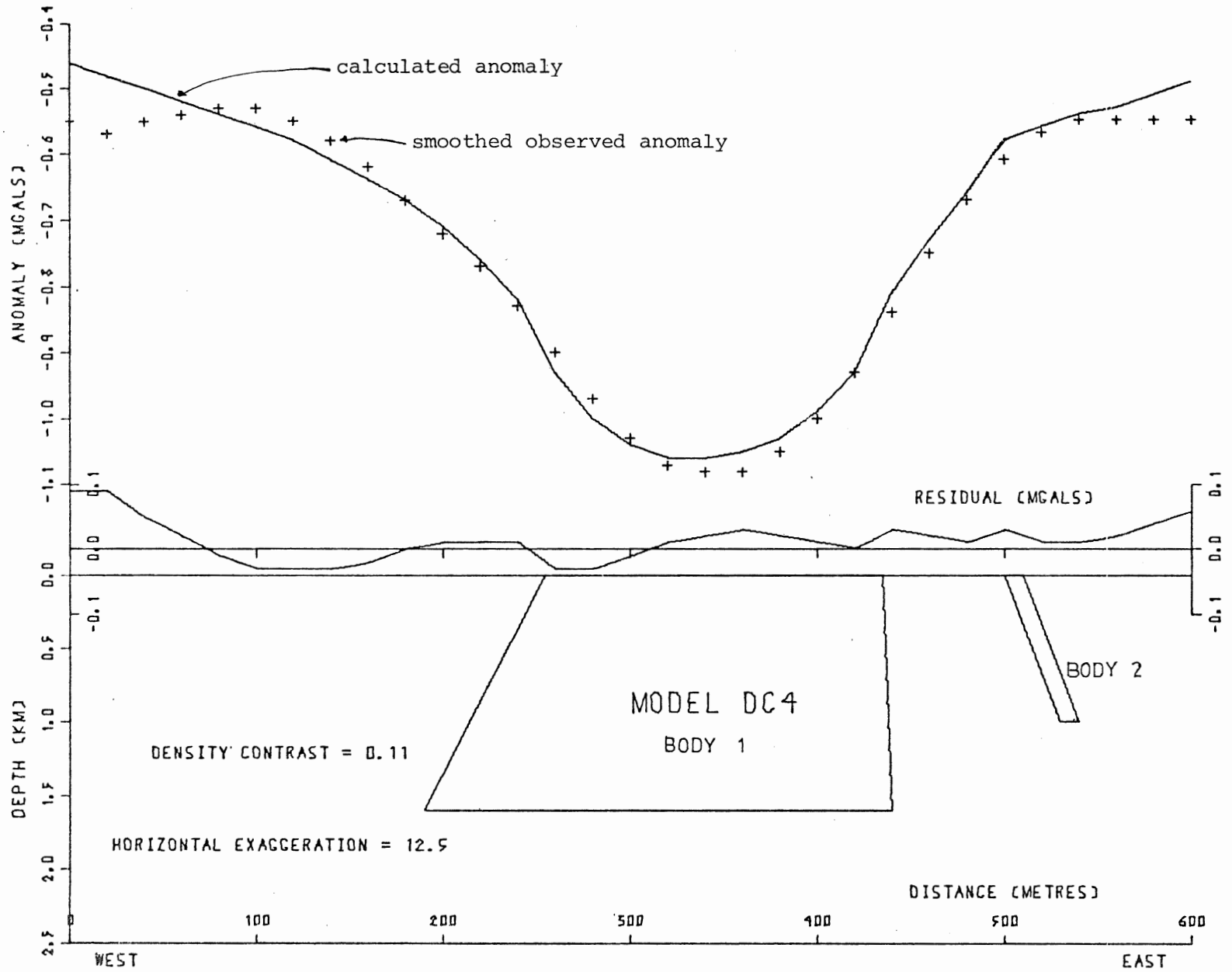

Figure 15. Gravity Model DC4, showing the basic unit sampled to the east of the intrusive. Body 1 has a density contrast of 0.11 g cm^{-3} with the surrounding volcanics; Body 2 has a density contrast 0.20 g cm^{-3} greater than the surrounding volcanics.

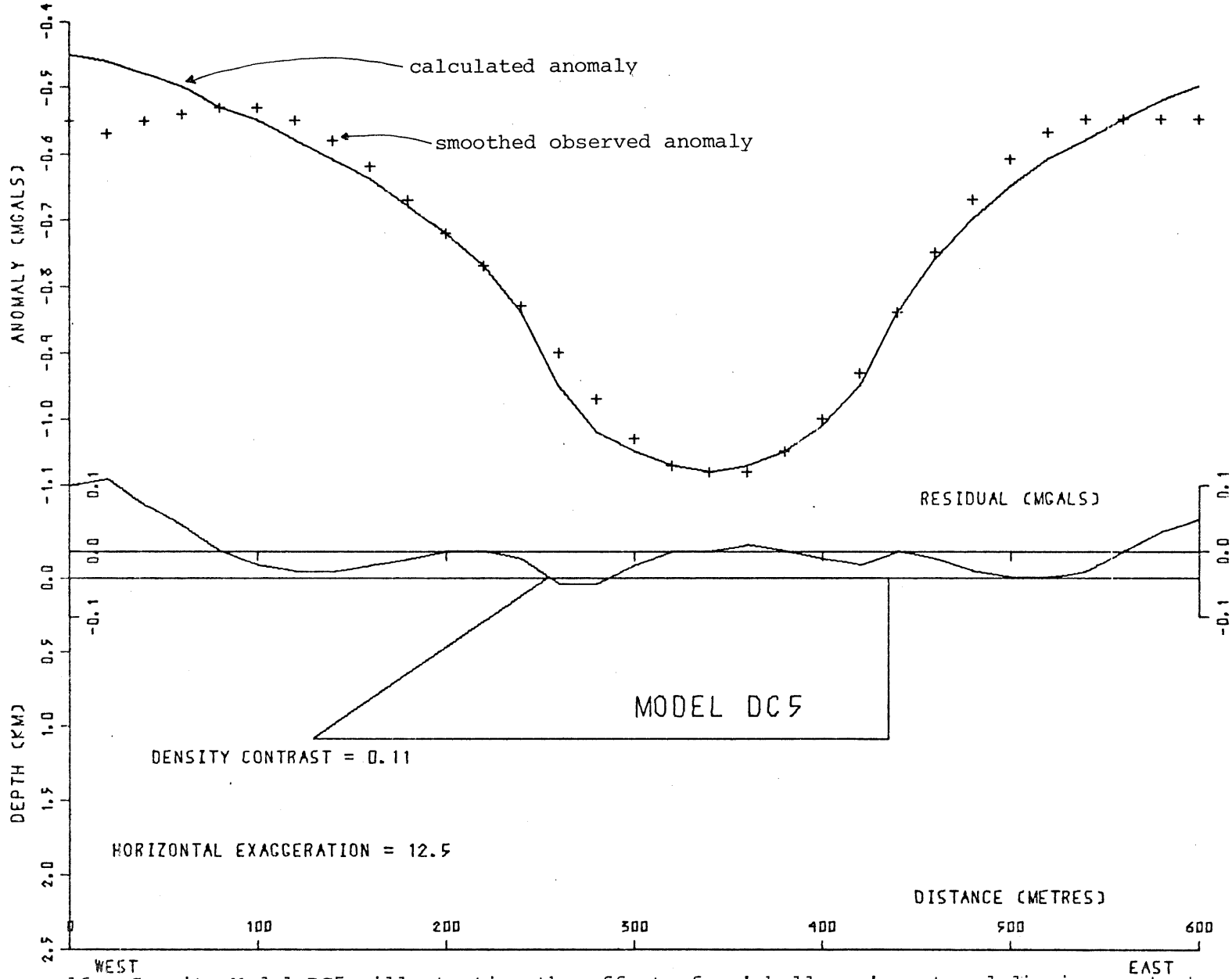

Figure 16. Gravity Model DC5, illustrating the effect of a 'shallower' westward dipping contact. The dip is about 84° to west, but appears shallower because of the horizontal exaggeration.

2) If the density contrast of the rock types is increased to greater than 0.13 g cm^{-3}, the effect is to increase the anomaly amplitude proportionately. If the depth is decreased to compensate for the greater density contrast, the resulting anomaly has too short a wavelength to match the observed data.

3) If shallower westerly dips are used (dips less than 80°), the low of the anomaly extends too far to the west (Figure 15).

4) When the depth to the bottom of the body is increased to greater than several kilometres, a smaller density contrast is required. However, the resulting anomaly is too wide to fit the observed data.

Magnetic Models

Only the induced component of magnetization was considered as the remanent contribution to the anomaly is quite small. The strength of the earth's field and its inclination were determined from U.S. Navy maps (U.S. Naval Oceanographic Maps, H.O. 1703 and 1700, 1966). A declination of 24°07' was interpolated for Deep Cove from the Mira 1:50000 topographic sheet (Mira Map Sheet, Department of Energy, Mines and Resources, Topographic Map 11F/16, 1975). The susceptibility contrast between the volcanic and intrusive rocks is 1.5×10^{-3} (cgs) as measured on the inductance bridge. The orientation of the survey line (considered to be 018°) relative to magnetic North needed to be taken into account.

In order to obtain a calculated anomaly which approximated the observed data, two alterations were needed:

1) In the gravity models the depth to the top of the body was assumed to be zero. However, the same model produced much too short a wavelength in the calculated magnetic anomaly (see Figure 17). To obtain an approximate match between the observed anomaly and the calculated anomaly, it was necessary to increase the depth to the top of the magnetic layer to 30 metres.

2) As the depth to the top of the body was increased, a higher magnetic susceptibility contrast (about 3 times the observed) was required to produce an anomaly of the observed amplitude.

Magnetic anomalies were calculated for the models which had already been used in the gravity modelling. These are shown in Figures 17 - 22. Figure 19 illustrates the effect of changing the susceptibility contrast from 3.7×10^{-3} to 4.6×10^{-3} (cgs), respectively, for Model DC-2.

Some modelling observations are:

1) The only models which can match the observed anomaly are models whose eastern boundary is shifted eastward. If the perturbing effect on the magnetic field is caused by the quartz monzonite body, such a shift would contradict field evidence and is not substantiated by the gravity data.

2) If the depth to the top of the 'magnetic body' is increased to broaden the calculated anomaly's wavelength, an unrealistic

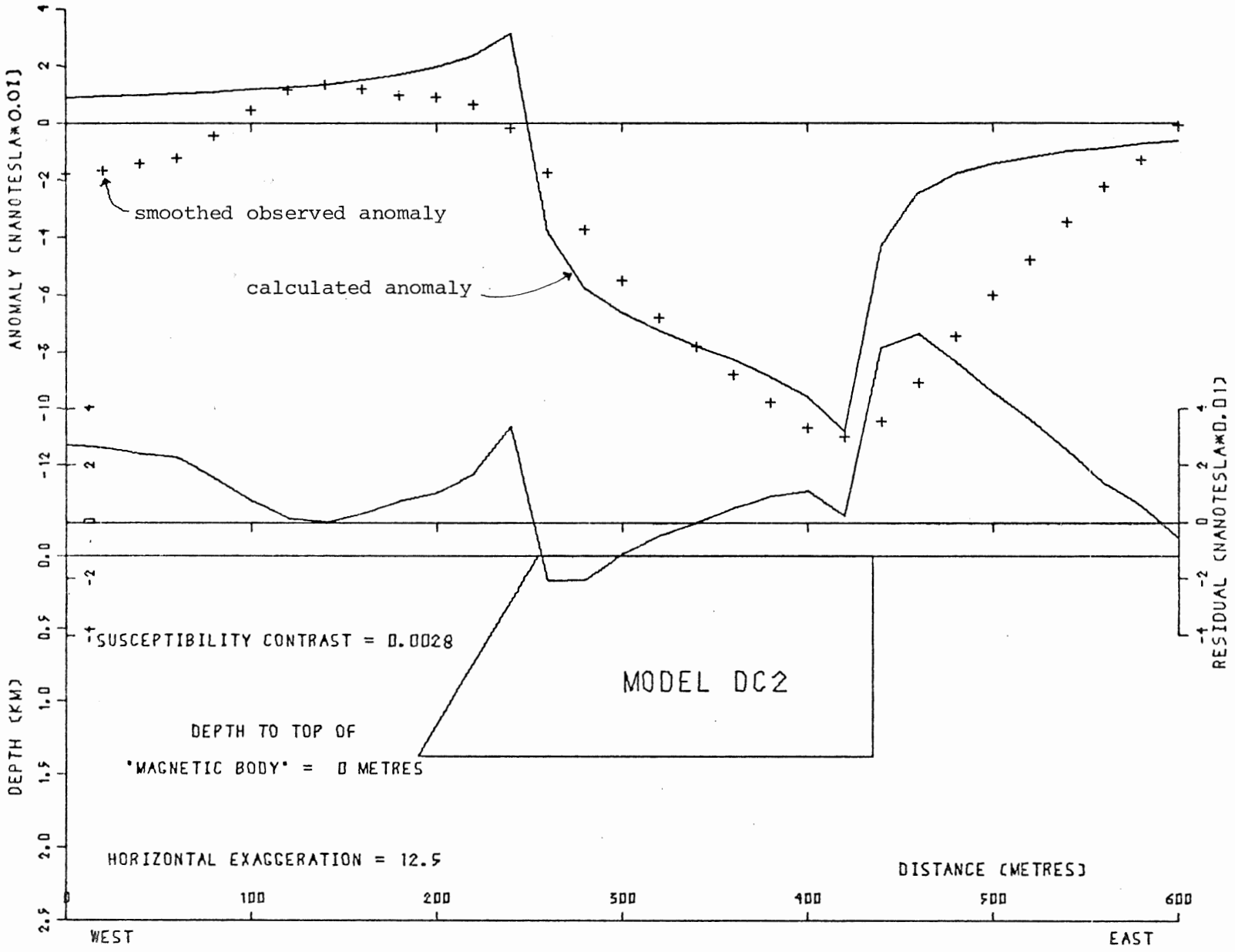

Figure 17. Magnetic Model DC2 illustrating the effect of considering the depth to top of 'magnetic body' of 0 metres. Note that the calculated anomaly peaks are far too sharp and its wavelength too short.

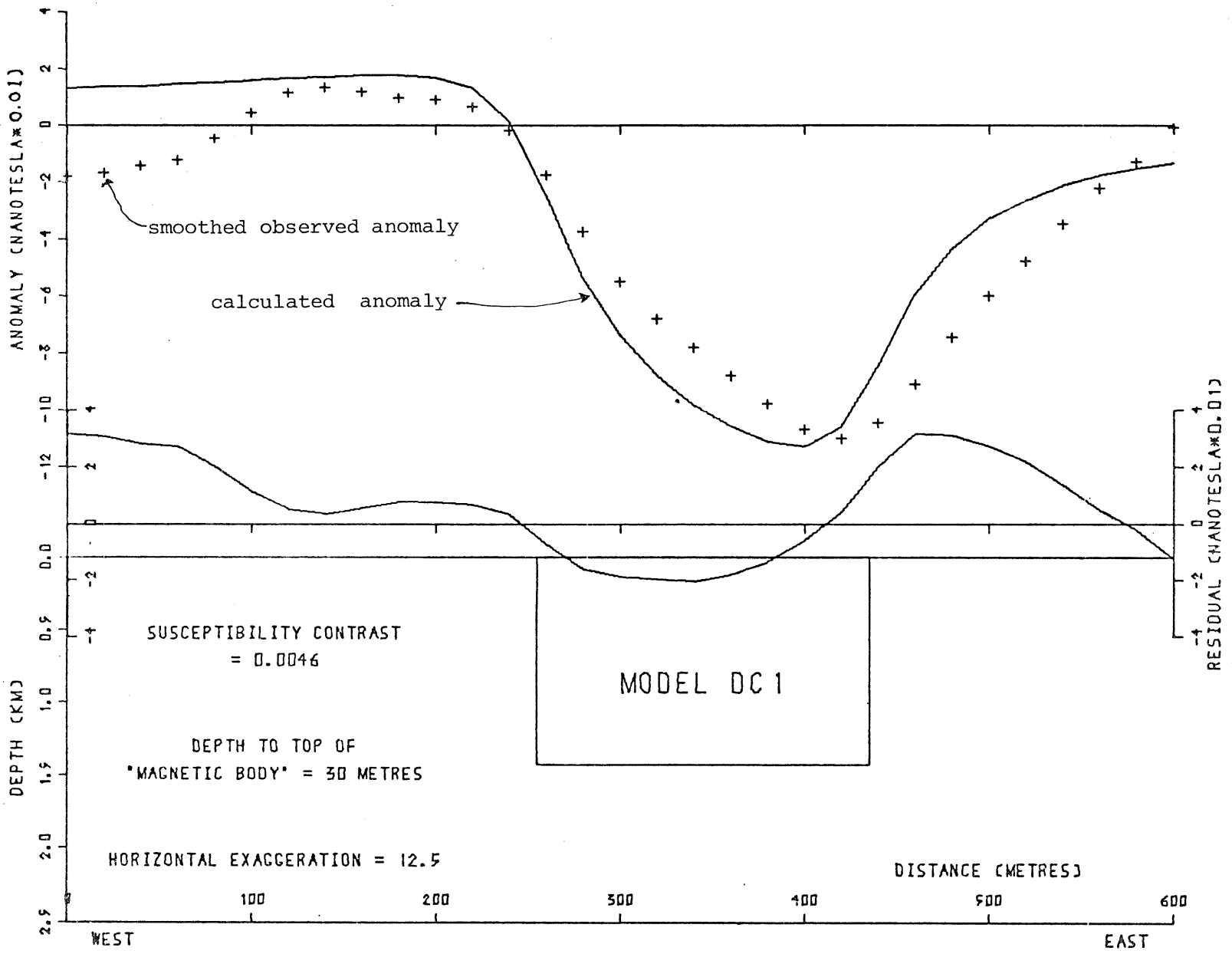

Figure 18. Magnetic Model DC1.

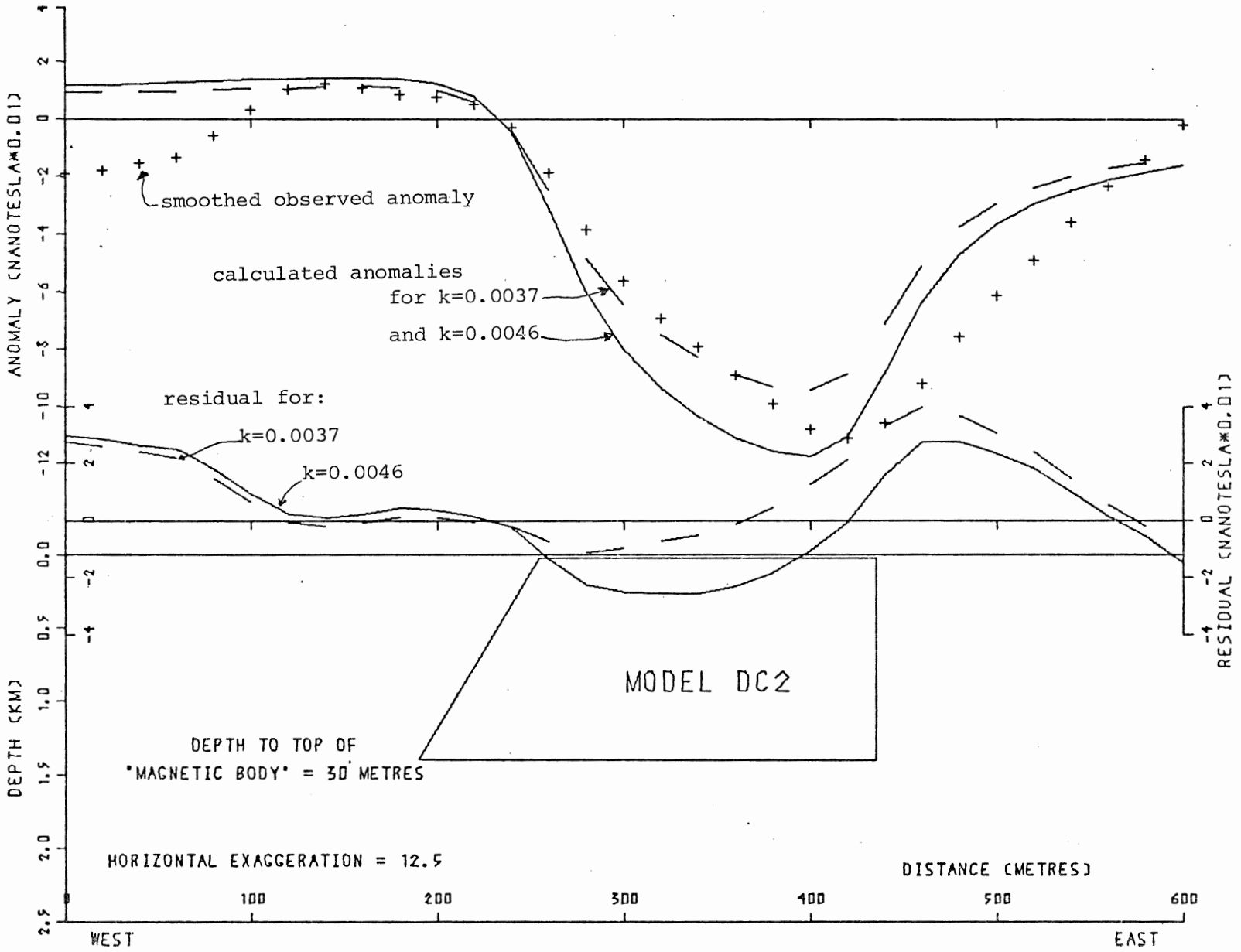

Figure 19. Magnetic model DC2, showing the effect of varying the susceptibility contrast from 3.7×10^{-3} to 4.6×10^{-3} as measured in cgs units.

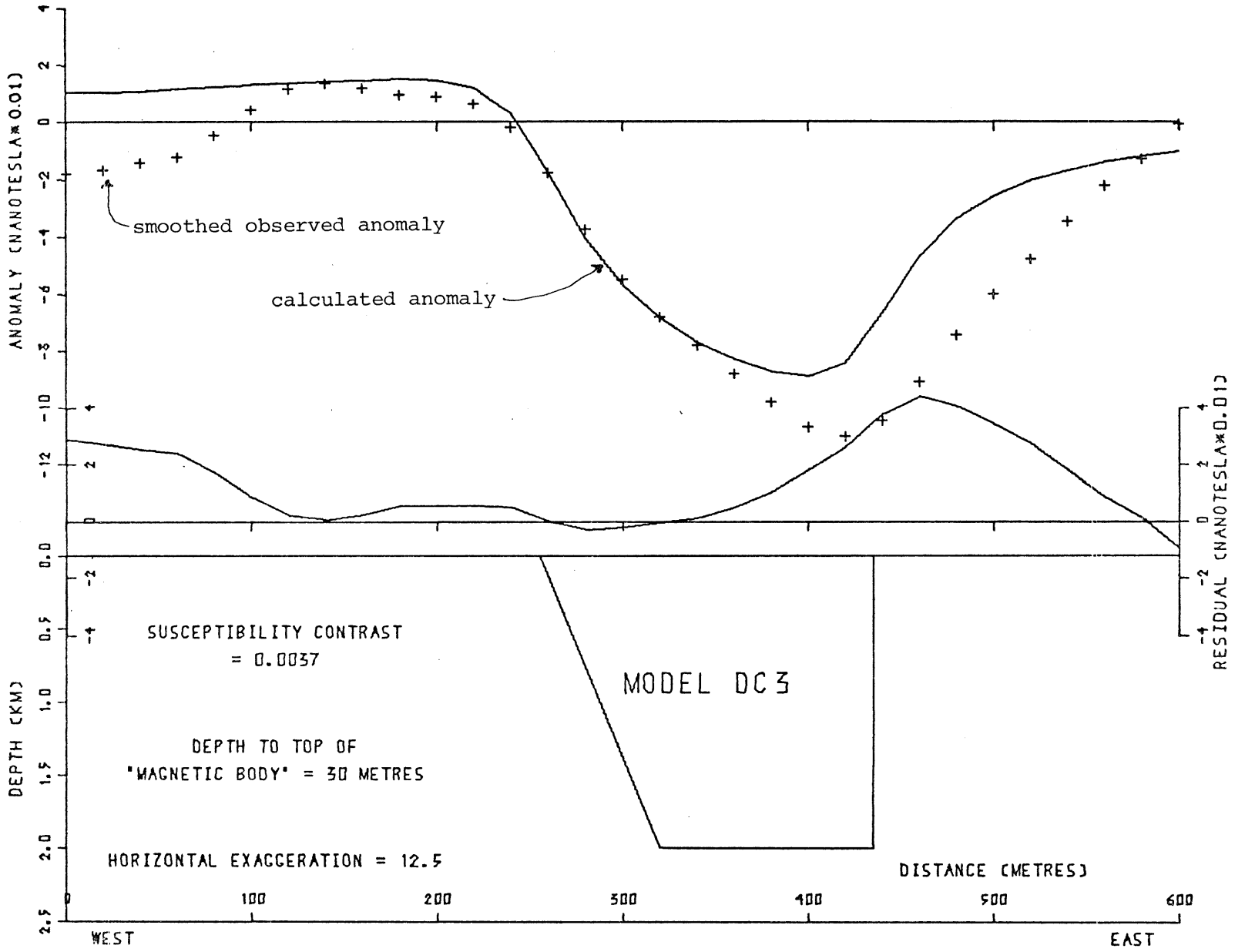

Figure 20. Magnetic Model DC3.

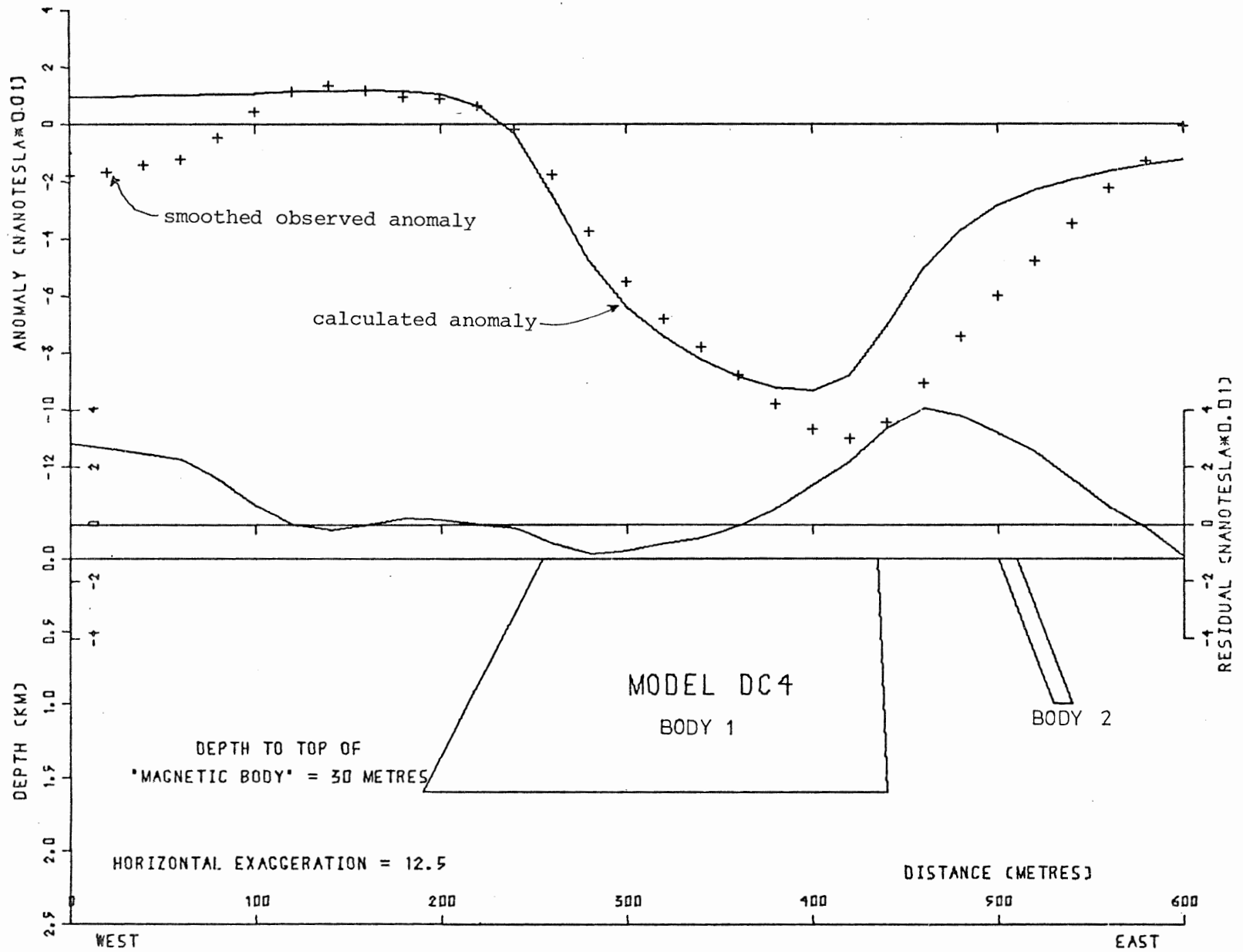

Figure 21. Magnetic Model DC4. Body 1 is considered to have a susceptibility contrast of 0.0037, Body 2 has a susceptibility contrast of 0.0009 (greater than the surrounding volcanics).

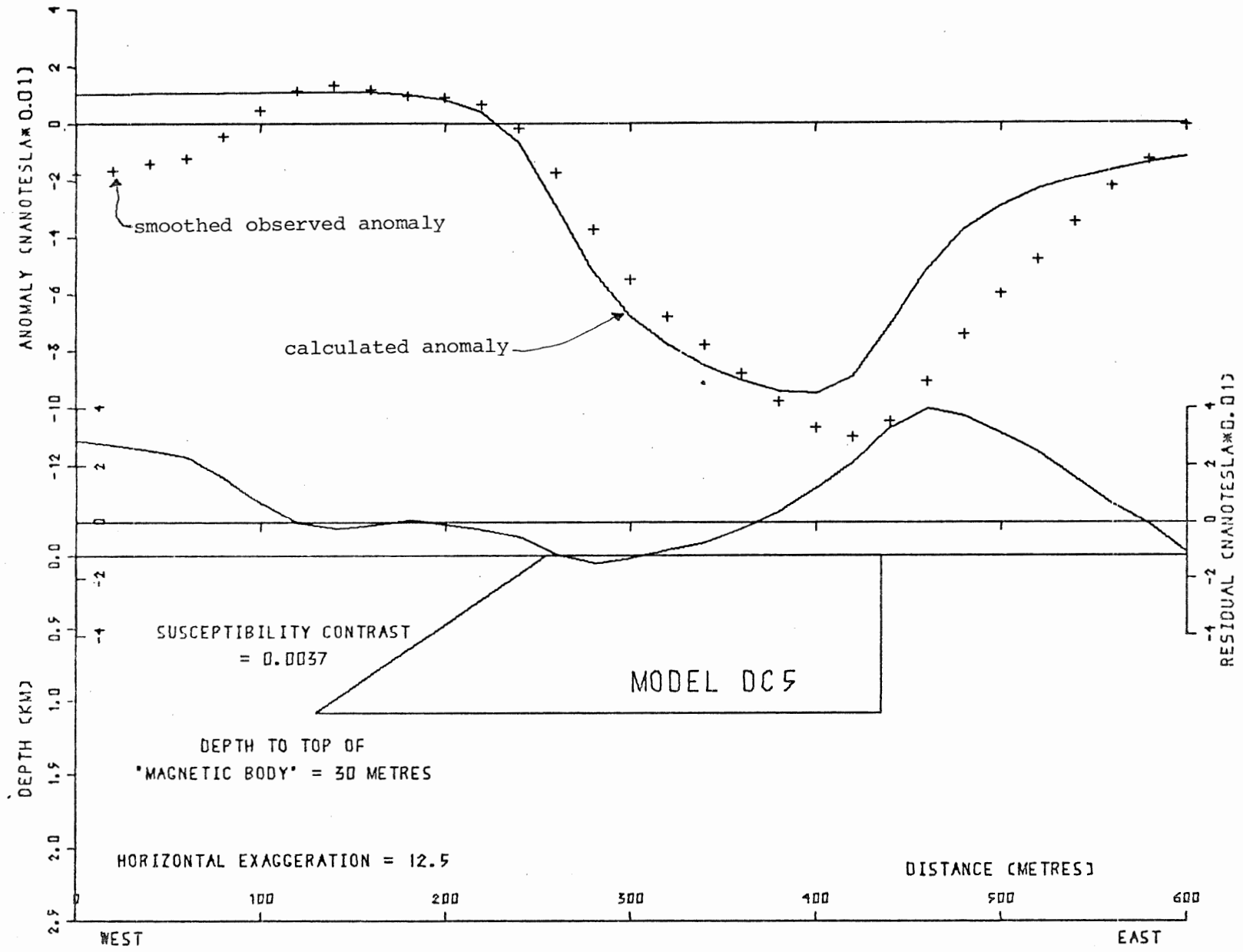

Figure 22. Magnetic Model DC5.

susceptibility contrast is required to produce an anomaly of the observed amplitude.

3) Variations in the angle of contacts and the depth to the bottom of the body have very little effect on the calculated anomaly.

4) Adding an upper layer with the observed susceptibility contrast has little effect on the calculated anomaly.

The significance of the 30 metre depth to the top of the 'magnetic body' is that the ferrimagnetic minerals have possibly weathered to minerals with lower susceptibilities in the uppermost volcanic rocks. Thus the susceptibility of the surface rocks as measured may be lower than the susceptibilities of deeper, less-weathered rocks. The effective 'magnetic body' producing the anomaly may, therefore, be at a depth of about 30 metres.

The magnetization of the volcanic rocks to the east of the intrusive may have been affected by contact metamorphism, resulting in an eastward shift of the boundary of the 'magnetic body' as is observed in the data. The absence of a corresponding westward shift of the west contact may be significant, perhaps indicating a post-intrusive fault contact along this boundary.

IX. Conclusions

The expected gravity and magnetic anomalies due to contrasting properties of the volcanic and intrusive rocks are observable in the survey data. These anomalies can be reasonably explained using simple, two-dimensional models, with field and laboratory observations as constraints.

The density of the quartz monzonite was determined to be 2.63 ± 0.01 g cm^{-3}. The average density of the volcanic rocks was considered to be between 2.73 and 2.78 g cm^{-3}.

The average magnetic susceptibility of the volcanic rocks tested in the laboratory is 1.5×10^{-3} in cgs units, whereas the susceptibility of the quartz monzonite was at least 100 times less.

The volcanic rocks at Deep Cove have Koenigsberger Q-ratios which are, in most cases, considerably less than unity. The direction of the remanent vectors of the volcanic rocks are highly variable. Therefore, remanent magnetization does not contribute significantly to the anomaly.

The magnetic anomaly indicates that the surface volcanic rocks may have a lower susceptibility than the deeper rocks, possibly because of weathering of ferrimagnetic minerals. The susceptibility may have also been lowered in the contact aureole surrounding the intrusive.

The calculated gravity anomalies of models which best fit the observed data near the west contact suggest that the contact is nearly

vertical, perhaps dipping steeply to the west. The magnetic anomalies are not very sensitive to the dip of the contact.

Only simple models are presented in this paper and, it should be reiterated, these are not the only models which will produce the observed anomaly. A more complex treatment of this subject would require additional geological constraints and would employ three-dimensional modelling methods.

References

Books and Articles

Bingley, J., 1967. Louisbourg Project, Cape Breton County, Nova Scotia, 1964-1967. Unpubl. Nova Scotia Dept. Mines Rept.

Cormier, R. F., 1972. Radiometric ages of granitic rocks, Cape Breton Island, Nova Scotia. Can. J. Earth Sci. 9, pp. 1074-1086.

Dobrin, M. B., 1976. Introduction to geophysical prospecting. McGraw-Hill Book Company, New York, 630 pp.

Douglas, J. K. and Prahl, S. R., 1972. Extended terrain correction tables for gravity reductions. Geophysics 37, pp. 377-379.

Grant, F. S. and West, G. F., 1965. Interpretation theory in applied geophysics. McGraw-Hill Book Company, New York, 584 pp.

Hammer, S., 1939. Terrain corrections for gravimeter stations. Geophysics 4, pp. 184-194.

Hollister, V. F., Potter, R. R. and Barker, A. L., 1974. Porphyry-type deposits of the Appalachian Orogen. Econ. Geol. 69, pp. 618-629.

Hutchinson, R. D., 1952. The stratigraphy and trilobite faunas of the Cambrian sedimentary rocks of Cape Breton Island, Nova Scotia. Geol. Surv. Can. Mem. 263.

International Mathematical and Statistical Libraries, Reference Manual: Subroutine ICSSCU

Lehman, N. E., 1976. Cape Breton porphyry copper-molybdenum prospects, Nova Scotia. Letter to St. Joseph's Exploration Ltd., 8 pp.

Mendenhall, W., 1971. Introduction to probability and statistics. Wadsworth Publishing Company, Inc., Belmont, California, 466 pp.

O'Reilly, G. A., 1977. Field relations and mineral potential of the granitoid rocks of southeast Cape Breton Island. Nova Scotia Dept. Mines Rept. 77, pp. 81-87.

Reinsch, C. H., 1967. Smoothing by spline functions. Numerische Mathematik 10, pp. 177-183.

Riddell, J. E., 1973. Report of 1972 operations, Gabarus Bay Project of United Asbestos Corporation Ltd. Nova Scotia Dept. Mines (open file), 81 pp.

Sangster, A. L., 1976. Deep Cove, Project 223: Report on mining claims. Nova Scotia Dept. Mines (closed file), 24 pp.

Scientific Subroutine Package, Programmer's Manual: Subroutine SRANK.

Streckeisen, A. L., 1967. Classification and nomenclature of igneous rocks: Final report of an inquiry. N. Jahrb. Miner. Abh. 107, pp. 144-240.

Talwani, M., Worzel, J. L. and Landisman, M., 1959. Rapid gravity computations for two-dimensional bodies with application to the Mendocino submarine fracture zone. J. Geophys. Res. 64, pp. 49-59.

Telford, W. M., Geldart, L. P., Sheriff, R. E. and Keys, D. A., 1976. Applied geophysics. Cambridge University Press, Cambridge, 860 pp.

Weeks, L. J., 1954. Southeast Cape Breton Island, Nova Scotia. Geol. Surv. Can. Mem. 277, 112 pp.

Wiebe, R. A., 1972. Igneous and tectonic events in northeastern Cape Breton Island, Nova Scotia. Can. J. Earth Sci. 9, pp. 1262-1277.

Maps

Canada Department of Energy, Mines and Resources. 1:50000 Topographic Map, Mira District, Nova Scotia, 11F/16, 1975.

Canada Department of Mines; Geological Survey of Canada. 1:63360 Aeromagnetic Map, Mira District, Nova Scotia, 11F/16, 1955.

Canada Department of Northern Affairs and National Resources; National Parks Branch. 1:7200 Topographic Map of Fortress of Louisbourg National Historic Park, Sheet # 4, 1962.

United States Oceanographic Office, Washington, D. C. Map of the Magnetic Inclination or Dip, Map H.O. 1700, 1965.

United States Oceanographic Office, Washington, D. C. Map of the Total Intensity of the Earth's Magnetic Force, Map H.O. 1703, 1965.

Appendix I

Elevations of Stations Relative to Station # 1

Station	Elevation (metres)
1	0.00*
2	0.47
3	0.25
4	0.00
5	0.81
6	1.31
7	1.63
8	1.79
9	2.62
10	3.19
11	2.40
12	2.62
13	3.21
14	4.47
15	6.04
16	7.10
17	8.08
18	10.53
19	11.76
20	12.73
21	14.00
22	13.76
23	12.59
24	11.89
25	11.88
26	11.36
27	11.56
28	11.45
29	12.22
30	12.90
31	12.23
32	11.79
33	10.64
34	8.75

* Determined from topographic maps to be approximately 9 metres above sea level.

Appendix II

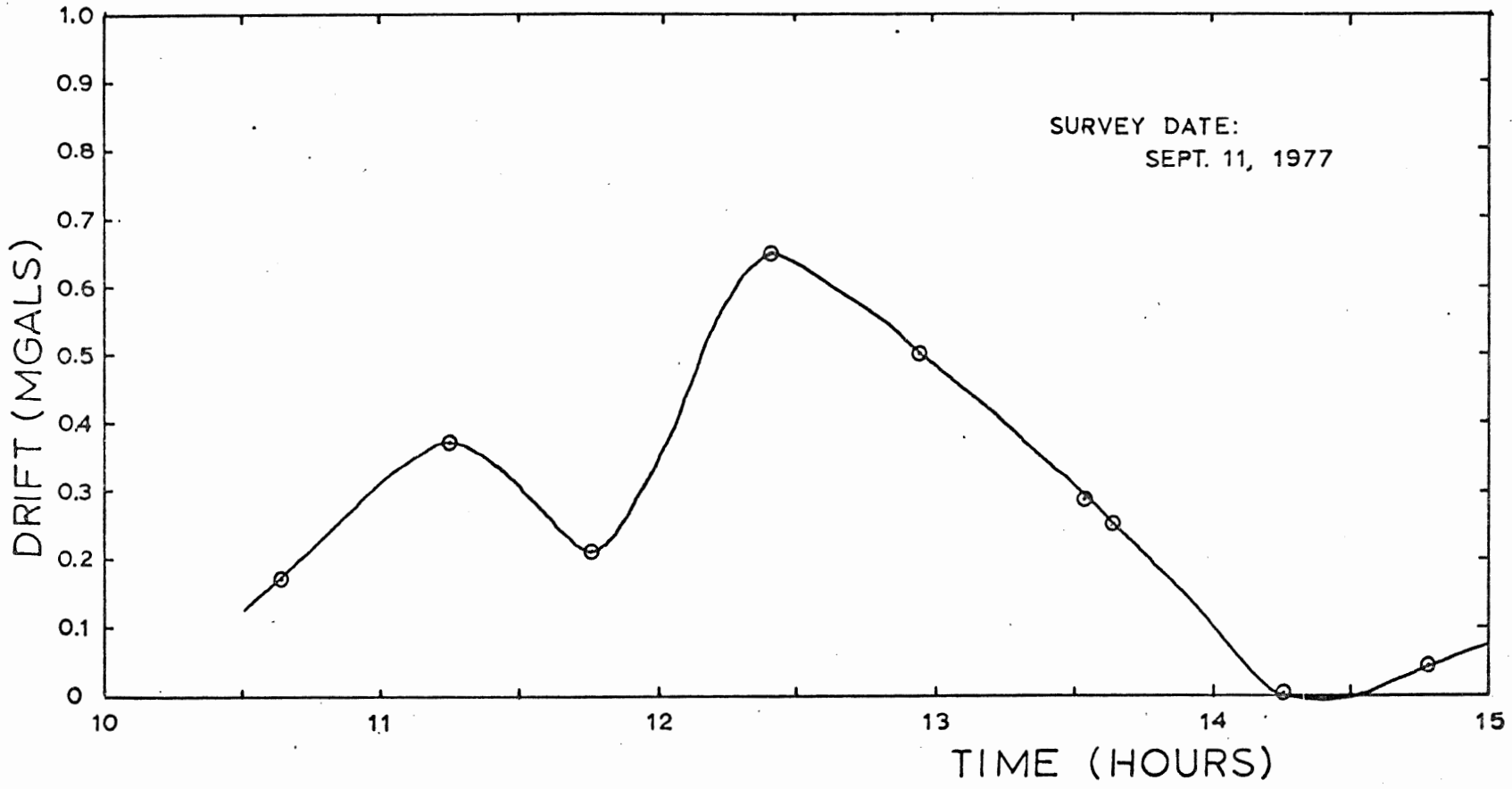

Gravity Meter Drift Curve

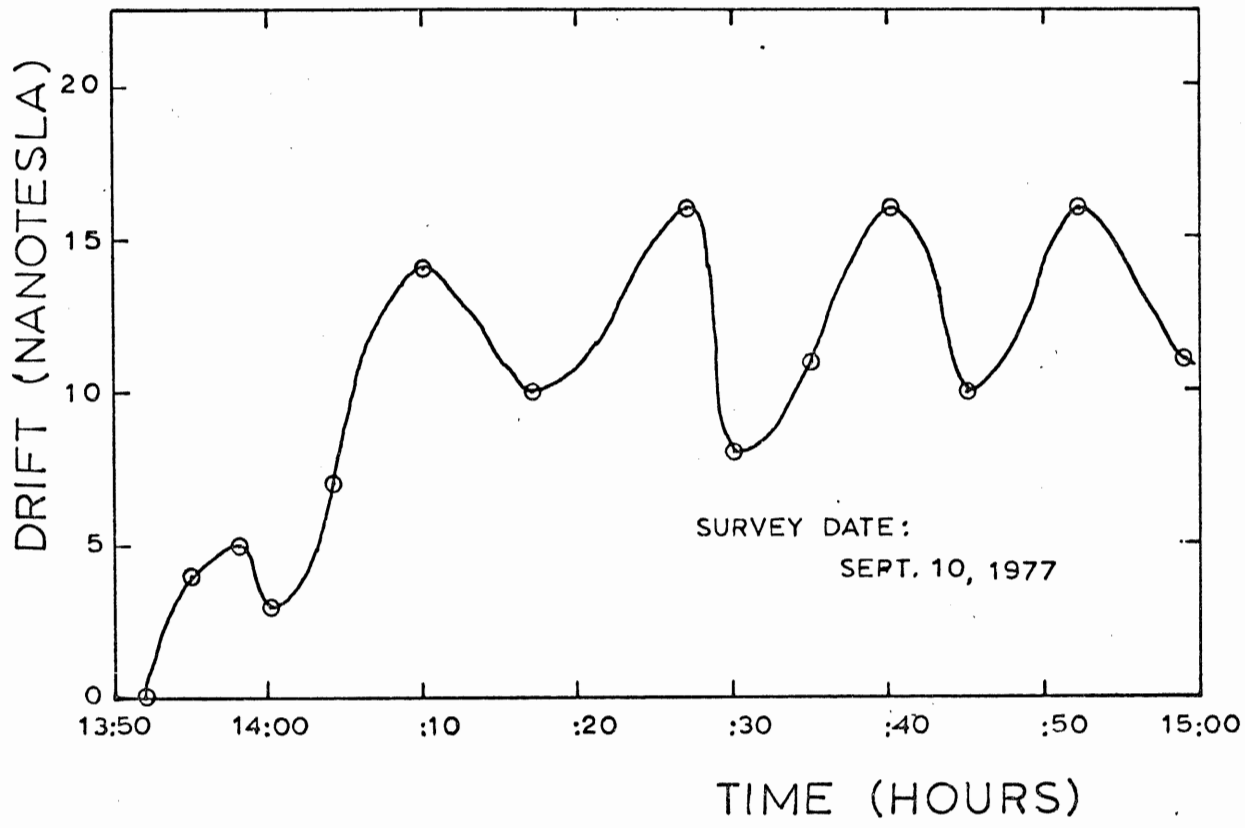

Magnetometer Drift Curve

Appendix III

Sample Densities and Descriptions

Sample	Density ($g\ cm^{-3}$)	Description
DC1	2.76	Andesite
DC2	2.63	Quartz Monzonite
DC3	2.55*	Granite, with potassic alteration
DC4	2.62	Quartz monzonite
DC5	2.62	Quartz monzonite
DC6	2.65*	Granite with phyllic alteration
DC7	2.72	Andesite
DC8	3.03	Basalt, with disseminated pyrite
DC9	2.78	Andesite
DC10	2.83	Andesite (float)
DC11	2.61	Quartz monzonite, fine-grained from dyke
DC12	2.96	Basalt, with disseminated pyrite
DC13	2.62	Quartz monzonite
DC14	2.74	Andesite
DC15	2.63*	Quartz monzonite with molybdenite from dyke
DC16	-	Vein sulphides, mainly pyrite and arsenopyrite
DC17	2.73	Andesite
DC18	2.73	Andesite
DC19	2.84	Andesite
DC20	2.86	Andesite
DC21	2.70	Rhyolite (near contact)
DC22		Missing sample
DC23	2.63	Quartz monzonite
DC24	2.60	Quartz monzonite
DC25	2.62	Quartz monzonite
DC26	2.93	Basalt, with disseminated pyrite
DC27	2.97	Basalt, with disseminated pyrite
DC28	2.71	Andesite
DC29	2.73	Andesite
DC30	2.64	Quartz monzonite
DC31	2.62	Quartz monzonite
DC32	2.60	Quartz monzonite
DC33	2.64	Quartz monzonite
DC34	2.63	Quartz monzonite
DC35	2.65	Quartz monzonite
DC36	-	Drilled Samples,
DC37	-	Broken on extraction
DC38	2.70	Andesite from trench
DC39	2.70	Andesite
DC40	2.76	Andesite

Sample Densities and Descriptions (continued)

Sample	Density ($g\ cm^{-3}$)	Description
DC41	2.64	Quartz monzonite, from dyke
DC42	2.68	Rhyolite
DC43	2.75	Andesite
DC44	2.76	Andesite
DC45	2.93	Basalt, with disseminated pyrite
DC46	2.62	Quartz monzonite
DC47	2.63	Quartz monzonite
DC48	2.64	Quartz monzonite
DC49	2.64	Quartz monzonite
DC50	2.63	Quartz monzonite
DC51	2.93	Basalt
DC52	2.65	Rhyolite
DC53	-	Extremely altered and mineralized sample from intrusive core.
DC54	2.78*	

* Not used in determining average density

Appendix IV

Magnetic Data of Oriented Samples

Definition of terms:

Demagnetization: Peak strength of alternating current washing field in Oe (1 Oe = 79.6 A/m in SI units)

Declination: Angle subtended in the horizontal plane between the remanent vector and true North.

Inclination: Angle subtended in the vertical plane between the remanent vector and the horizontal.

$|\vec{J}|$ = magnitude of remanent vector (Oe)

K = magnetic suceptibility in cgs units

$|\vec{I}|$ = magnitude of induced magnetization caused by the present earth's field, $\vec{H}$ (Oe). $|\vec{I}| = K|\vec{H}|$

Q = Koenigsberger ratio = $\frac{|\vec{J}i|}{|\vec{I}|}$ where $|\vec{J}i|$ is the strength of the original remanent vector of a sample

Sample	Demagnetization (Oe)	Declination (degrees)	Inclination (degrees)	J (Oe)	K (in cgs units)	I (Oe)	Q
DC26	0	47.8	75.8	2.94×10^{-5}	1.6×10^{-4}	8.7×10^{-5}	0.34
	25	96.7	73.9	2.06×10^{-5}			
	50	124.4	71.2	1.86×10^{-5}			
	75	123.0	49.6	$1.84\ 10^{-5}$			
DC-27	0	200.5	64.6	7.84×10^{-5}	7.5×10^{-4}	4.1×10^{-4}	0.19
	25	186.9	62.2	6.62×10^{-5}			
	50	186.0	58.6	5.50×10^{-5}			
	75	197.5	67.2	4.11×10^{-5}			
	100	185.3	70.5	3.05×10^{-5}			
	150	179.0	64.7	2.58×10^{-5}			
	200	215.2	69.1	1.56×10^{-5}			
DC-28	0	93.9	64.7	1.06×10^{-4}	1.3×10^{-3}	7.1×10^{-4}	0.15
	25	100.3	77.3	7.44×10^{-5}			
	50	139.2	81.1	5.65×10^{-5}			
	75	149.1	78.8	5.61×10^{-5}			
	100	139.2	73.8	3.09×10^{-5}			
	150	94.2	57.8	2.34×10^{-5}			
	200	95.4	44.8	1.17×10^{-5}			
DC-29	0	-0.3	57.5	1.01×10^{-5}	2.7×10^{-3}	1.5×10^{-3}	0.07
	25	-6.2	55.3	8.42×10^{-5}			
	50	-7.9	55.6	7.47×10^{-5}			
	75	-6.7	56.0	6.21×10^{-5}			
	100	-4.8	58.5	5.36×10^{-5}			
	150	-4.9	58.9	3.65×10^{-5}			
	200	-3.2	63.6	2.99×10^{-5}			
	250	-0.9	62.8	1.75×10^{-5}			
	300	-6.1	69.7	1.23×10^{-5}			
	350	-5.8	69.6	9.56×10^{-6}			

Sample	Demagnetization	Declination	Inclination	J (Oe)	K (in cgs units)	I (Oe)	Q
DC30	0	20.8	27.5	1.82×10^{-7}	$\approx10^{-5}$	$< 10^{-5}$	0.07
	25	38.6	28.0	1.67×10^{-7}			
	50	23.2	24.6	1.84×10^{-7}			
	75	10.6	25.5	1.98×10^{-7}			
	100	11.4	32.8	1.81×10^{-7}			
DC38	0	2.5	60.2	2.44×10^{-5}	7.3×10^{-4}	4.0×10^{-4}	0.61
	25	0.3	58.0	2.53×10^{-5}			
	50	-4.1	57.7	2.47×10^{-5}			
	75	-3.8	59.3	2.27×10^{-5}			
	100	-5.7	64.3	2.16×10^{-5}			
	150	-7.8	65.6	1.85×10^{-5}			
	200	-12.5	62.9	1.47×10^{-5}			
	250	0.3	60.9	1.43×10^{-5}			
	300	-0.8	69.3	1.30×10^{-5}			
	350	1.4	66.7	1.10×10^{-5}			
	400	-8.4	71.2	1.04×10^{-5}			
	500	-20.2	73.5	8.92×10^{-6}			
	600	1.0	75.8	8.02×10^{-6}			
DC39	0	87.3	71.9	7.83×10^{-5}	2.0×10^{-3}	1.1×10^{-3}	0.07
	25	99.7	80.2	6.01×10^{-5}			
	50	101.3	81.5	4.59×10^{-5}			
	75	121.5	82.2	3.65×10^{-5}			
	100	133.4	79.4	2.83×10^{-5}			
	150	120.9	76.4	2.24×10^{-5}			
	200	85.9	83.3	1.40×10^{-5}			
	250	72.9	76.0	1.04×10^{-5}			
	300	55.7	76.0	9.06×10^{-6}			
	350	58.4	69.7	9.55×10^{-6}			
	400	38.7	64.9	7.53×10^{-6}			

Sample	Demagnetization	Declination	Inclination	J (Oe)	K (in cgs units)	I (Oe)	Q
DC44	0	-2.7	38.8	5.57×10^{-5}	1.5×10^{-3}	8.1×10^{-4}	0.07
	25	52.8	86.2	2.32×10^{-5}			
	50	74.4	52.5	1.67×10^{-5}			
	75	47.6	-2.8	2.43×10^{-5}			
	100	0.4	-20.9	1.34×10^{-5}			
	150	147.8	-16.2	1.33×10^{-5}			
	200	169.1	-7.5	1.10×10^{-5}			
	250	193.8	-12.3	1.08×10^{-5}			
	300	261.8	-10.8	5.68×10^{-6}			
DC45	0	161.9	68.3	3.15×10^{-3}	3.7×10^{-3}	2.0×10^{-3}	1.6
	25	177.3	58.5	2.56×10^{-3}			
	50	181.8	52.9	1.70×10^{-3}			
	75	179.5	47.7	1.12×10^{-3}			
	100	178.1	49.9	7.79×10^{-4}			
	150	169.1	47.5	5.25×10^{-4}			
	200	173.7	45.1	3.47×10^{-4}			
	250	165.0	48.6	3.87×10^{-4}			
	300	160.9	44.3	2.32×10^{-4}			
	350	147.5	54.4	2.09×10^{-4}			
	400	203.5	21.3	9.80×10^{-5}			
	500	183.5	35.4	2.20×10^{-4}			
	600	131.8	-4.9	9.93×10^{-5}			